DEUTSCHES ELEKTRONEN – SYNCHROTRON

DESY 90-156
FTUAM-EP-90-03
December 1990

Heavy Quark Physics in ep Collisions at LEP+LHC

A. Ali

Deutsches Elektronen-Synchrotron DESY, Hamburg

F. Barreiro, J.F. de Trocóniz

Universidad Autónoma de Madrid, Spain

G.A. Schuler

II. Institut für Theoretische Physik, Universität Hamburg

J.J. van der Bij

Institute for Theoretical Physics, University of Amsterdam

ISSN 0418-9833

NOTKESTRASSE 85 · D-2000 HAMBURG 52

To be sure that your preprints are promptly included in the HIGH ENERGY PHYSICS INDEX , send them to the following address (if possible by air mail) :

DESY
Bibliothek
Notkestrasse 85
2 Hamburg 52
Germany

DESY 90-156
FTUAM-EP-90-03
December 1990

ISSN 0418-9833

Heavy Quark Physics in ep Collisions at LEP+LHC[1]

A. Ali

Deutsches Elektronen Synchrotron DESY
Hamburg, Fed. Rep. Germany

F. Barreiro, J.F. de Trocóniz

Universidad Autónoma de Madrid, Madrid, Spain

G.A. Schuler[2]

II Inst. f. Theor. Phys. der Universität Hamburg
Hamburg, Fed. Rep. Germany

J.J. van der Bij

Inst. voor Theor. Fysica, Univ. van Amsterdam
Amsterdam, The Netherlands

[1]To be published in the Proceedings of the ECFA Workshop on LHC, Aachen, FRG (1990).
[2]Supported by BMFT, under contract 054HH92P/3, Bonn, FRG.

Abstract

We study electroweak production of heavy quarks- charm, beauty, and top- in deep inelastic electron-proton collisions at the proposed LEP+LHC collider at CERN. The assumed energy for the collisions is $E_e = 50$ GeV, $E_p = 8000$ GeV, providing an ep center of mass energy, $\sqrt{s} \simeq 1.26\ TeV$. We invoke the boson-gluon fusion model to estimate theoretical cross sections and distributions for the heavy quarks. Higher order QCD corrections are only approximately taken into account, by assuming a (normalization) K-factor of 2 for the charm and beauty quark production rates and incorporating the parton shower cascades. With these assumptions and the parametrization of Eichten et al. for the structure functions (EHLQ, set 1), we find the following cross sections: $\sigma(ep \to c+X) \simeq O(3\ \mu b)$, $\sigma(ep \to b+X) \simeq O(40\ nb)$, and $\sigma(ep \to t+X) \simeq 4\ pb$ for $m_t = 120$ GeV, decreasing to 0.5 pb for m_t =250 GeV. These cross sections would provide $O(6 \times 10^9)$ charmed hadrons, $O(8 \times 10^7)$ beauty hadrons, and $O(10^3)$ top hadrons, for an integrated ep luminosity of 1000 pb^{-1}. The heavy quark rates in ep collisions are considerably smaller than the corresponding rates in pp collisions at LHC, with $\sqrt{s} = 16$ TeV. This gives a clear advantage to pp collisions for top searches. However, for the charmed and beauty quarks only a tiny fraction of the cross sections in $p+p \to Q+X$ can be triggered in comparison to the corresponding cross sections in $e+p \to Q+X$, resulting in comparable number of measured heavy quark events in the ep and pp mode. We sketch the energy-momentum profile of heavy quark events in ep collisions and illustrate the kind of analyses that experiments at the LEP+LHC collider would undertake to quantitatively study heavy quark physics. In particular, prospects of measuring the particle-antiparticle mixing parameter $x_s = \Delta M/\Gamma$ for the $B_s^0 - \bar{B}_s^0$ meson system are evaluated, and search strategies for the top quark in ep collisions are presented.

1 Introduction

Heavy flavour physics is one of the central themes of high energy colliders. It is fair to say that Quantum Chromodynamics (QCD) provides an adequate account of heavy quark production at present colliders [1]. These comparisons will become more quantitative in the forthcoming experiments at Tevatron ($p\bar{p}$) and HERA (ep). The interest in the charmed and beauty physics at future colliders lies mainly in the hopes that the anticipated high rates could be advantageously used to do high precision physics, including rare decays and possibly CP violation. In exploring the potential of c- and b- quark physics at the LEP+LHC collider we have, therefore, concentrated on those aspects which could be characterized as search for new phenomena which may possibly be studied in ep collisions.

The situation with the top quark is, however, quite different with the top quark becoming more and more conspicuous due to its continued absence. Hence the primary goal is to find the top quark and measure its mass with a reasonable accuracy. Unfortunately, the present lower bound on the top quark mass, $m_t \geq 91$ GeV [2], and indirect mass estimates from the electroweak radiative corrections yielding $m_t = 140 \pm 40$ GeV [3]-[6], have pushed the top quark discovery threshold beyond the reach of the presently operating and about to be commissioned accelerators in Europe. This list includes the CERN colliders, $Sp\bar{p}S$, LEP(I), LEP(II), and the ep collider HERA at DESY. In the foreseeable future the Fermilab $p\bar{p}$ collider is best poised for bagging the top quark [7]. Future pp colliders, SSC and LHC, have robust rates for even (unrealistically) heavy quarks [1], [8]–[12], and hence hadron colliders are the most natural habitat of the elusive top quark. The potential of an ep collider, such as LEP+LHC, is of exploratory nature as far as top quark physics is concerned.

We argue here that a top quark with a mass less than or equal to 200 GeV can be produced and discovered in ep collisions at the LEP+LHC collider. This optimism is based on theoretical calculations for the two relevant production mechanisms $e + p \to \nu + \bar{t} + b + X$ and $e + p \to e + t + \bar{t} + X$, shown in Fig. 1. The integrated cross sections for the two processes and their sum as a function of the top quark mass are shown in Fig. 2. They have been calculated for ep collisions with $E_e = 50$ GeV and $E_p = 8000$ GeV, giving $\sqrt{s} \simeq 1.26\ TeV$. With an integrated luminosity of 1000 pb^{-1} these cross sections yield $\sim$ 3500 top quark events for $m_t = 120$ GeV, with the rate decreasing to $\sim$ 500 events for $m_t = 250$ GeV. Top quarks in the standard model decay mainly via $t \to b + W^+$, giving rise to the dominant final state $e + p \to \nu + b + \bar{b} + W^- + X$, involving a W boson and a pair of $b\bar{b}$ quarks. With the above mentioned rate estimates, we undertake two complementary analyses based on the decay $\bar{t} \to \bar{b} + W^-$, followed by the leptonic decay $W^- \to l^- + \nu_l$ and the hadronic decay $W^- \to q + \bar{q}'$. The former decay would give rise to the final state containing a (b-quark)-jet, an l^-, and large missing transverse momentum, $\not{p}_\perp$. We shall call this analysis the semileptonic top quark analysis. The latter decay mode of the top quark would give rise to multijet final states, emanating from the 3-parton decay $t \to b + W^+ \to b + q + \bar{q}'$, and we call this the hadronic top quark analysis.

An estimate of the number of background events in ep collisions at the LEP+LHC collider at $\sqrt{s} \simeq 1.26\ TeV$ for an assumed luminosity of 1000 pb^{-1} is given in Table 1 (section 2). Though the background from the deep inelastic charged current CC and neutral current NC processes (both low and high Q^2), as well as from the c- and b- quark production is huge in comparison with the expected number of top quark events, this can be brought down to a tolerable level by imposing a series of topological and kinematic cuts, which are detailed

in the text. We remark that the hardest background in both the semileptonic and hadronic analysis emerges from the processes in which a $W^\pm$ is radiated off the lepton or the quark line. The production of a real W^- boson, with or without additional jet(s), gives rise to event topologies in which the top quark signals are being sought. Not surprisingly, the real W-events directly produced (background) and the ones emerging as secondary particles in top quark decays (signal) behave qualitatively similarly.

To improve the signal to background (S/B) ratio, one may have to demand b-quark tagging as the top quark production always leads to $W^- + b + \bar{b}$ or $W^+W^- + b + \bar{b}$ events. Since the directly produced $W^\pm X$ background events are expected to be poor in b-quark, b-tagging is going to play a crucial role for top quark searches. In the anlayses presented below, we impose b-tagging by demanding a charged lepton inside a jet (i.e., not isolated lepton) having $p_\perp > 5$ GeV. This improves the S/B ratio, but at a considerable cost of top quark events. This reduction in rate could be overcome if one could use a microvertex detector, which, for instance in the context of photoproduction of charmed hadrons, has so successfully been used to suppress the dominant background due to the light quarks at lower energies [13]. In Tables 3 and 4 we take the reader through a myriad of kinematic cuts, to suppress the background in top quark searches. It is clear from these tables, that the LEP+LHC collider would have a sensitivity (at $\geq 5\sigma$ level) to the top quark for $m_t \leq 200$ GeV. The hadronic analysis provides a good estimate of the top quark mass through the invariant mass of the 3-jets coming from top decays, where the jets have been defined by a typical algorithm, such as the one used by the UA1 collaboration. To simulate experimental conditions, we have smeared the invariant mass distributions of the jets with a Gaussian function of width $\Delta m_t = 15$ GeV. The resulting distributions still allow to observe the invariant mass peak due to the top quark.

We now turn to the discussion of charmed and beauty quark physics in ep collisions at the LEP+LHC collider. To simulate their production and decays we have used the Monte Carlo programme AROMA [14], which was developed for heavy flavour studies at HERA. We caution that there are considerable uncertainties in the theoretical underpinning of the event generator being used and hence in the projections presented here. They pertain in part to the gluon density, which would be probed at HERA and LEP+LHC colliders at very small x-values. There are good arguments to expect that the gluon density at small-x would show a certain saturation behaviour due to the QCD non-linear evolution effects [15]–[18]. This behaviour is hard to quantify at this stage and we have used the conventional approach in the evolution of the parton densities [19], [20]. In part, the uncertainties are also due to the presence of large logarithm terms like $(\alpha_s \log(4m_Q^2/s))^n$ in $\sigma(ep \to Q + X)$ [21], [22], which will have to be resummed in all orders –something which has not yet been accomplished. We also remark that colour coherence influences the attendant partonic radiation accompanying the $Q\bar{Q}$ pair in $e + p \to Q + X$ events [23], an effect which has still to be incorporated in the programme being used.

We content ourselves here with incorporating the QCD corrections by an effective K-factor, which increases the $e + p \to Q + X$ cross section, evaluated in the lowest non-trivial order, by K=2 for both $\sigma(ep \to c + X)$ and $\sigma(ep \to b + X)$. For the structure functions we use the EHLQ (set 1) parametrization [24], with the number of quark flavours $n_f = 5$ in both the parton evolution and α_s. With these inputs we determine : $\sigma(ep \to c + X) = 2.8\ \mu b$, $\sigma(ep \to b + X) = 40$ nb at $\sqrt{s} \simeq 1.26\ TeV$. These rates should be contrasted with the corresponding estimated rates $\sigma(ep \to c + X) \sim 1\ \mu b$ and $\sigma(ep \to b + X) \sim$ 10 nb, at HERA with $\sqrt{s} = 314$ GeV [25]. The estimated increase in cross sections between the HERA and

LEP+LHC energies is a factor ~ 3 for $\sigma(ep \to c + X)$, and a factor ~ 4 for $\sigma(ep \to b + X)$. With an integrated luminosity of 1000 pb^{-1}, one would have $\sim 6 \times 10^9$ charmed hadrons and $\sim 8 \times 10^7$ beauty hadrons in ep collisions at LEP+LHC. These potentially large rates could be put to good use if one has a dedicated ep detector, having good particle identification, energy momentum resolution, and a functional microvertex detector.

Note that the cross-sections for producing the charmed and beauty hadrons in ep collisions at the LEP+LHC collider though large are no where close to the corresponding cross-sections in $p+p \to Q+X$ at LHC, which are estimated to be: $\sigma(pp \to c+X) \sim O(1\ mb)$ and $\sigma(pp \to b+X) \sim O(100\ \mu b)$. Thus, the rates in ep collisions at LEP+LHC are typically 3-4 orders of magnitude smaller than at LHC(pp) with $\sqrt{s} = 16$ TeV. The large rates in the pp mode are not necessarily an advantage, since rates of ~ 10 MHz for the charmed hadrons and ~ 1 MHz for the beauty (for a luminosity of $10^{34} cm^{-2} s^{-1}$ in pp collisions) can not possibly be triggered. So, only charmed and beauty hadron events with large transverse momentum will actually be measured in pp collisions. Since the cross sections at LEP+LHC are smaller and the intended ep luminosity typically $10^{32} cm^{-2} s^{-1}$, the charmed and beauty quark events in ep collisions will have a frequency of ~ 300 Hz and ~ 4 Hz, respectively, which are probably measurable without much data reduction. We expect that the trigger conditions may lead to comparable measured cross sections for the charmed and beauty hadrons in the ep (LEP+LHC) and the pp (LHC) modes.

Production of heavy quarks in ep collisions would allow a very precise measurement of the gluon structure function, in particular at very small values of the x_g-variable, where x_g is the fractional energy of the proton that a gluon carries. Because of the impending interest in the small-x_g region, it would be worthwhile to use the charm and beauty hadrons as sensitive probes of the new QCD dynamics. We calculate the rates for some useful heavy quark final states in ep collisions and find that a trigger, based on the transverse hadron energy of say 10 GeV measured in the pseudorapidity interval $|\eta| \leq 3$, would make x_g-values as small as 10^{-5} accessible at the LEP+LHC collider. If in addition, a charged lepton (electron or muon) having $p_\perp^l \geq 1$ GeV is required as a heavy quark tag, then still x_g- values as small as $\sim 6 \cdot 10^{-5}$ would be reachable. Likewise, the process $e + p \to J/\psi + X$ has rather large cross-section. Using the dileptons from J/ψ decays to trigger on heavy quarks, it has been estimated in an accompanying report, that x_g-values as small as $3 \cdot 10^{-5}$ could be measured in ep collisions at LEP+LHC [26]. These issues will be studied at HERA with the view of measuring the gluon saturation effects. The larger energy at LEP + LHC would allow to probe the gluon structure function at an order of magnitude smaller x_g-values.

There is one specific issue that we have investigated for the process $e + p \to b + X$, namely the decay length distributions of the beauty hadrons and the prospects of measuring oscillation length for the $B_s^0 - \bar{B}_s^0$ transition. We recall here that the ratio $x_d = \Delta M/\Gamma$ for the $B_d^0 - \bar{B}_d^0$ system has already been measured by the ARGUS and CLEO collaborations [27], [28] with the result: $x_d = 0.65 \pm 0.13$. This is a landmark measurement in b-physics. The corresponding ratio for the $B_s^0 - \bar{B}_s^0$ transition, x_s, is expected to be very large, with present expectations dispersed in the range $3 \leq x_s \leq 30$. Measuring x_s is going to be a hard nut to crack, not only for experiments at the ep colliders but at any collider [29]-[35]. It is now generally agreed that the measurement of x_s may require at least $O(10^7)$ beauty hadrons, which is attainable in ep collisions at the LEP+LHC collider with an integrated luminosity of 1000 pb^{-1}. The real question is how many of these events will survive the trigger conditions, and how many of the B_s^0-hadrons can actually be identified and/or reconstructed.

We recall that at present only time integrated information on the mixing measures $\chi_i = x_i^2/2(1 + x_i^2)$, i=d,s, is available. The weighted mixing average $\chi = \chi_d P_d + \chi_s P_s$ (with P_d and P_s being the branching ratios for $b \to B_d$ and $b \to B_s$, respectively) has been measured in a number of e^+e^- annihilation and $p\bar{p}$ collision experiments. Some representative measurements of χ are [36]:

$$\chi = 0.160 \pm 0.040 \pm 0.020 \quad \text{(UA1)}$$
$$\chi = 0.130 \pm 0.045 \quad \text{(ALEPH)}$$
$$\chi = 0.178 + 0.049 - 0.040 \quad \text{(L3)}$$

In particular, the L3 collaboration has quoted a lower bound: $\chi_s > 0.14$ at 90% confidence level [37]. These measurements will very likely be improved at LEP [43], Tevatron [38] and HERA [25]. The improvement of the statistical errors in χ may allow to check the expectations in the standard model $\chi_s \sim 0.5$, but it may not allow a meaningful determination of the quantity x_s, partly due to the model dependent branching ratios P_d, P_s, but more importantly due to the (theoretically expected) large value of x_s, for which deviations from perfect mixing, $\propto (1/2 - x_s^2/2(1+x_s^2))$, become quadratically insensitive to x_s. One may be forced to measure the time-dependent oscillation phenomena, i.e. oscillation lengths, to be able to determine x_s. The oscillation lengths of a hadron may be defined as:

$$\lambda_{osc} = (2\pi/x)\gamma\beta c\tau \tag{1}$$

where γ and β are the Lorentz factors, and $c\tau = 300\ \mu m$ for beauty hadrons. Note that λ_{osc} is inversely proportional to the mixing ratio $x_i, i = d, s$, in contrast to the quadratic dependence of χ_i on x_i. The only measurable oscillating component in the decay lengths is expected to be due to the $B_s^0 - \bar{B}_s^0$ transition. The point is that the oscillation length for the $B_d^0 - \bar{B}_d^0$ transition is just too long to be measurable; all other B-hadrons (except B_s) decay exponentially. So, one has to measure the small but characteristic sinusoidal (oscillating) component against a large and (almost) exponentially falling background. In doing this, one has to separate the time evolution of the right-sign meson, i.e. $B_s \to B_s$, and the wrong-sign meson, $B_s \to \bar{B}_s$, since otherwise no deviation from the background would be seen. This would require B_s-tagging in some functional form. We have not investigated the all important question of the efficiency of B_s-meson tagging and the resulting precision on the B_s hadron energy, which are the real limiting factors in estimating the error on the proper time resolution. A detector-oriented detailed study has to follow our first estimates here to ascertain whether or not the $O(10^7)$ $e + p \to b + X$ events anticipated at the LEP+LHC collider are sufficient to measure x_s, and the attainable accuracy.

The final states which we have analysed here are the same in which most of the mixing phenomena in the $B^0 - \bar{B}^0$ sector todate have been observed in time integrated experiments, namely the same sign and opposite sign dileptons. The differential (in length) distributions for the processes $e + p \to b + \bar{b} + X \to l^\pm l^\pm + X$ and $e + p \to b + \bar{b} + X \to l^\pm l^\mp + X$, after subtraction of the background, should show the sinusoidal behaviour characteristic of the $B_s^0 - \bar{B}_s^0$ oscillation. For this study we have assumed a (Gaussian distributed) resolution of 100 μm in the reconstruction of decay length - a requirement which a microvertex detector should easily be able to meet. Since the error on proper time arises also from the error on the B-hadron momentum, this has to be measured with a reasonable accuracy (say 10 %). The result for the opposite sign dileptons with the (assumed) indicated B-hadron energy binning and $x_s = 10$ is shown in Fig. 23. The main difficulty in determining x_s via dilepton final states is the (anticipated) large error in the determination of the B-hadron energy and

it is very likely that the experimental distributions would be smeared over a much larger energy range than what we have assumed in our study, thereby degrading the nice oscillating patterns being shown here. Consequently, the relative error $\Delta x_s/x_s$ that one could get from this method could be rather large. Nevertheless, it will be a determination of x_s. Of course, at some point all the sensitivity will be lost if x_s is very large, say $x_s \geq 15$, since the oscillations would become too fine grained to be resolved.

The paper is organized as follows. Section 2 describes the estimates of the heavy quark cross sections in ep collisions at the LEP+LHC collider. Strategies for the top quark search using the semileptonic and hadronic final states are also presented in this section. Section 3 contains an energy momentum profile of the charmed and beauty hadrons at the LEP+LHC collider , including estimates of the decay lengths for the beauty hadrons and (x_s)-dependent oscillation lengths. The measurements of the gluon density at very small values of x_g using inclusive lepton final states is also taken up in this section; the inclusive J/ψ-production in this context is being discussed elsewhere [26]. We conclude with a summary in section 4.

2 Top Quark Searches at LEP(I)+LHC

2.1 Estimates of cross sections

In QCD, the leading order contribution to heavy quark production is due to the boson-gluon mechanism shown in Fig. 1 [39]-[42]:

$$CC : W^- + g \rightarrow \bar{t} + b;\ \bar{c} + s, ... \tag{2}$$

$$NC : \gamma/Z\ +\ g \rightarrow \bar{t} + t;\ \bar{b} + b;\ \bar{c} + c \tag{3}$$

giving rise to the processes

$$e(l_e) + p(P) \rightarrow \nu_e(l') + \bar{Q}(p'_f)\ +\ Q'(p_f) + X \tag{4}$$

$$e(l_e) + p(P) \rightarrow e(l') + \bar{Q}(p'_f)\ +\ Q(p_f) + X \tag{5}$$

where the 4-momenta of the particles are indicated. The definition of the kinematic variables follows the standard notation:

$$\hat{s} = (p_f + p'_f)^2 \tag{6}$$

$$Q^2 = -q^2 = -(l_e - l')^2 \tag{7}$$

$$W^2 = (P + q)^2 \tag{8}$$

$$x = \frac{Q^2}{2P.q} \tag{9}$$

$$y = \frac{P.q}{p.l_e} \tag{10}$$

with the obvious relations

$$Q^2 = xys \tag{11}$$

$$W^2 = Q^2\frac{(1-x)}{x} + m_p^2 \tag{12}$$

NC	CC	νW^-	eW^-	$c\bar{c}$	$b\bar{b}$
$4.3 \cdot 10^9$	$2.4 \cdot 10^5$	960	$2.8 \cdot 10^4$	$2.8 \cdot 10^9$	$4 \cdot 10^7$

Table 1: Expected number of background events in ep collisions at the LEP+LHC collider with an integrated luminosity of 1 fb^{-1}. The cuts are explained in the text.

$$\hat{s} = Q^2\frac{(x_g - x)}{x} \tag{13}$$

and x_g has been defined earlier. Note that $x_g \gg x$, in general.

The Monte Carlo generator AROMA [14], used in the calculations, is based on leading order QCD calculation for the production and weak decays of heavy quarks. The NC and CC processes (for both low and high Q^2) have been simulated using the event generators AROMA [14] and LEPTO [48]. As already stated in the introduction, higher order QCD corrections have been only approximately taken into account by using the K-factors: $K(b\bar{b}) = K(c\bar{c}) = 2$, and implementing the parton shower cascades. Note, that we have set $K(b\bar{t}) = K(t\bar{t}) = 1$. Furthermore, the DIS events have been generated with the cuts $Q^2 \geq 5\ GeV^2$, $x \geq 10^{-4}$ and $W^2 \geq\ 5GeV^2$; and the light quark production at low Q^2 has been incorporated using the processes: $\gamma/Z + g \rightarrow q\bar{q}$; $\gamma/Z + q \rightarrow qg$, with the cuts $(p_\perp)_q > 1\ GeV$, $Q^2 < 5\ GeV^2$.

The calculations presented here are rather similar to the ones undertaken for heavy quark studies at HERA[25] -with obvious differences. These lie in the higher energy at the LEP+LHC collider ($E_e = 50\ GeV, E_p = 8\ TeV, \sqrt{s} \simeq 1.26\ TeV$) compared to HERA ($\sqrt{s} = 0.314\ TeV$), and in the decay pattern of the top quark, which with $m_t \geq m_W$ now decays via $t \rightarrow b + W^+$, giving rise to a 2-body state, as compared to the 3-body decays $t \rightarrow (q\bar{q}, l^+\bar{\nu}_l) + b$, which were assumed for the top quark searches at HERA. The events at the LEP+LHC collider involving top quark decay products would then have the final state configurations:

$$ep \rightarrow eW^+W^-b\bar{b}X \tag{14}$$

$$ep \rightarrow \nu W^-b\bar{b}X \tag{15}$$

Consequently, one has to take into account real $W^\pm$ production including parton cascades and fragmentation to estimate this background. Estimated rates for the heavy quarks, charm and beauty, and the background events for the NC, CC and real W^- production processes, νW^- and eW^-, are shown in Table 1, for an integrated luminosity of $1 fb^{-1}$. These numbers correspond to the assumed value of the electromagnetic fine structure constant $\alpha^{-1} = 127$, quark masses $m_c = 1.5\ GeV$, $m_b = 5.0\ GeV$, and ep energy $\sqrt{s} \simeq 1.26\ TeV$.

The expected numbers of top quark events for the same integrated luminosity for some representative values of the top quark mass are shown in Table 2.

The cross section $\sigma(ep \rightarrow \bar{t}X)$ for the top quark mass range $120\ GeV \leq m_t \leq 250\ GeV$ is plotted in Fig. 2, where the separate contributions from the NC process (γ/Z) and the CC process (W^-) are also shown. It is clear from Fig. 2 that for the plotted m_t range, the CC process $W^- + g \rightarrow \bar{t}b$ dominates, due to the (larger) available phase space, as compared to the NC process $\gamma/Z + g \rightarrow \bar{t}t$. For the central value $m_t = 140\ GeV$ (hinted by the electroweak data analysis), $\sigma(ep \rightarrow \bar{t}X) = 2.5\ pb$, becoming approximately 0.5 pb for $m_t = 250\ GeV$.

In what follows, we outline top quark search strategies for an assumed top quark mass, $m_t = 150\ GeV$, for which we expect 2000 events/fb^{-1}. The analyses presented here are based

$m_t(GeV)$	120	150	175	200	225	250
number of events	3500	2050	1380	950	670	475

Table 2: Expected number of top quark events in ep collisions at the LEP+LHC collider with an integrated luminosity of 1 fb^{-1}.

Cuts	CC	W^-	$c\bar{c}$	$b\bar{b}$	$top(150)$	$top(200)$	$top(225)$
$\Sigma E_\perp > 20\ GeV$	$2.3 \cdot 10^5$	$2.6 \cdot 10^4$	$2.4 \cdot 10^7$	$4.0 \cdot 10^6$	1971	937	662
$p_\perp^l > 8\ GeV$	1810	7170	$9.16 \cdot 10^4$	$9.17 \cdot 10^4$	833	429	303
$E_{acc}(0.4) < 1\ GeV$	–	6275	–	$1.37 \cdot 10^4$	444	204	144
$\not{p}_\perp > 15\ GeV$	–	6050	–	3	415	193	137
$N_{jet}(\lvert\eta\rvert < 2) \geq 1$	–	1925	–	1	325	141	96
$p_\perp^{l_2} > 5\ GeV$	–	21	–	–	82	44	31

Table 3: Expected number of background events from the indicated processes and top quark events for an integrated luminosity of 1 fb^{-1}, decaying semileptonically at the LEP+LHC collider with $\sqrt{s} \simeq 1.26\ TeV$. The kinematic cuts on the events are indicated and the successive cuts are cumulative. The background from the NC process is completely removed by demanding a lepton with $p_\perp^l > 8\ GeV$, and hence not shown here.

on both the CC top quark production process, $e + p \to \nu + \bar{l} + b + X$, and the NC process, $e + p \to e + t + \bar{t} + X$. However, we note that $\sigma(\bar{t}b) \gg \sigma(\bar{t}t)$. The top quark decays via $\bar{t} \to W^- + \bar{b}$, followed by either $W^- \to l^- + \nu_l$, giving rise to the $jet + l^- + \not{p}_\perp$ configuration, or by the hadronic decay $W^- \to q + \bar{q}'$, giving rise to 3-jet events.

We shall make use of various cuts to enhance the S/B ratio, which are specific to each search strategy. Note, that in all the analyses we have assumed the beam pipe cut to be 100 mrad, and in the analysis of the NC background, a cut on Q^2, $Q^2_{NC} \leq 10\ GeV^2$, is assumed, which is also applied to the $t\bar{t}$ production, which, of course, does not significantly reduces the top rate. The latter cut has been chosen, since for larger values of Q^2, the scattered electron will be detected, allowing the subtraction of such events. A cut in the visible transverse energy $\Sigma E_\perp \geq 20\ GeV$ is also imposed, which suppresses the background without significantly compromising the top signal.

2.2 Semileptonic Analysis for Top Quark Search

Here the charged lepton (e^- or μ^-) with the largest $p_\perp$ is used as the top quark tag. The large energy release in top quark decay contributes to events with high $p_\perp^l$, with $p_\perp^l$ measured w.r.t. the beam axis. We find that a cut on $p_\perp^l$ of the hardest lepton in the event, $p_\perp^l \geq 8\ GeV$, completely removes the NC(light quark) background and reduces the contribution from the CC events, $c\bar{c}$ and $b\bar{b}$ events by one to two orders of magnitude. However, this cut affects the real $W^- \to l^- + \nu_l$ events and top quark sample more or less in a similar way. This is shown in Fig. 3 and the numbers of events surviving this cut are displayed in Table 3.

In order to further suppress the $c\bar{c}, b\bar{b}$ and CC events we invoke a lepton isolation cut, which

is defined by introducing a cone centred around the lepton momentum in the pseudorapidity η and azimuthal angle ϕ space. Defining

$$\Delta R \equiv \sqrt{(\Delta\eta)^2 + (\Delta\phi)^2} \leq R_c \tag{16}$$

a lepton is considered as isolated if the transverse enery within the cone of size R_c is less than a given number. Our isolation criterion is: $E_\perp^{acc}(R_c = 0.4) \leq 1\ GeV$. This cut completely removes the $c\bar{c}$ and CC events, with the $b\bar{b}$ events reduced to about 15%. Understandably, the lepton isolation cut leaves the $W^- \to l^-\nu_l$ events practically intact and removes about 50% of the top events. At this stage, the $b\bar{b}$ and W-event samples constitute the largest background, as shown in Table 3.

The cut that is most effective in removing the $b\bar{b}$ events is the one on the missing transverse energy, $\not{p}_\perp^{cut}$. The point is that the dominant source of top events is the CC process, $e + p \to \nu + \bar{t} + b + X$. Thus for the signal, there are three sources of $\not{p}_\perp$, namely the scattered neutrino, the neutrino coming from the t decays and the beam pipe cut. In contrast, $b\bar{b}$ events are produced by the neutral current process $\gamma/Z + g \to b\bar{b}$, and for these events the distribution in $\not{p}_\perp$ falls off very sharply. We find that < 10 $b\bar{b}$ events survive for $\not{p}_\perp^{cut} = 15\ GeV$. At this point the only background that remains is from the real W-boson production processes but unfortunately it is very large, giving an S/B ratio of 415/6050!

The S/B ratio can be brought to a significant level if one demands a jet, i.e. looks for the configuration $l^- \not{p}_\perp + jet(s)$. Defining the jets using the UA1 jet algorithm with the jet-cone size $R_{jet}(\Delta\eta, \Delta\phi) = 0.7$ and having a minimal transverse energy $\Sigma E_\perp \geq 7\ GeV$, the jet multiplicity in the pseudorapidity interval $|\eta_j| < 2$, for the $t\bar{t}, b\bar{t}, b\bar{b}$ and W^-X events is shown in Fig. 4. One should draw attention to the very appreciable differences in the pseudorapidity distributions of the $e + p \to t + X$ and real W-production processes, due to the central production mechanism of the former and the fact that in the latter, the W-boson is radiated mainly from a quark line, which produces the W-bosons preferentially in the forward (i.e. proton-) direction. This effect can be seen quantitatively in Fig. 5, where we show the pseudorapidity distributions in the interval $|\eta| < 3$ for the topology of interest involving one-jet events. Demanding N(jets) ≥ 1, with the jet(s) contained in the pseudorapidity interval of $|\eta_j| < 2$ would remove about 2/3 of the W^-X events, whereas $\sim 80\%$ of the top quark events would survive, resulting in the ratio $\frac{S}{B} = \frac{325}{1925}$, for $m_t = 150$ GeV.

The final improvement of the S/B ratio can now be achieved if one requires b-quark (jet) tagging, since the top production and decay processes involve $W^+W^-b\bar{b}$ and $W^-b\bar{b}$ states. A useful (though by no means very efficient) b-tagging can be achieved by looking for lepton(s) inside a jet. This amounts to searching for the top quark in the dilepton final states, where one of the leptons is from the W-decay and the second one from the b-quark decay. Demanding that the second lepton satisfies a $p_\perp^l$-cutoff of 5 GeV, the S/B ratio becomes 82/21 for $m_t =$ 150 GeV, becoming 44/21 for $m_t =$200 GeV, as shown in Table 3. This would be sufficient to establish the existence of the top quark, but unfortunately the semileptonic analysis does not allow a very meaningful determination of m_t, for which we turn to the hadronic analysis.[1]

[1] In the ep group summary report of these proceedings by R. Rückl (vol. 1),the preliminary conclusions about top quark searches were drawn from an analysis in which the eW-production background was not adequately taken into account. As shown here, this is the most significant background to top searches in ep collisions and hence additional kinematic cuts and analyses had to be done to reduce it. This has resulted in smaller S/B ratios (substantially for the semileptonic analysis but also for the hadronic), which are given in Tables 3 and 4 here.

Cuts	CC	W^-	$c\bar{c}$	$b\bar{b}$	$top(150)$	$top(200)$	$top(225)$
$\Sigma E_\perp > 120\ GeV$	$3.6 \cdot 10^4$	$1.4 \cdot 10^4$	$1.6 \cdot 10^4$	3300	1110	675	505
$S_{cm} > 0.25$	1046	2716	935	230	668	267	150
$N(jets) \geq 3$	701	2394	928	228	650	255	142
$\not{p}_\perp > 30\ GeV$	680	690	30	7	500	190	110
$N_{jet}(\lvert\eta\rvert < 3) = 3$	540	500	15	3	190	90	50
$N_{jet}(\lvert\eta\rvert < 3) = 4$	115	170	12	3	192	76	42
$p_\perp^l > 5\ GeV$	30	65	6	3	166	80	45

Table 4: Expected number of background events from the indicated processes and top quark events, decaying hadronically, at the LEP+LHC collider at $\sqrt{s} \simeq 1.26\ TeV$ and an integrated luminosity of 1 fb^{-1}. The kinematic cuts on the events are indicated and the successive cuts are cumulative. The NC process has been removed by the cuts: $S_{cm} > 0.25$, $\Sigma E_\perp > 120\ GeV$, $\not{p}_\perp > 30\ GeV$ and hence not shown. The last cut corresponds to the minimal b-tagging, discussed in the text.

2.3 Hadronic Analysis for Top Quark Search

Searches for the top quark in this section are based on the hadronic decays of the top quark

$$ep \to \nu\bar{l}bX \Rightarrow q\bar{q}'b\bar{b}X \tag{17}$$

$$ep \to e\bar{t}t \to eW^+W^-b\bar{b}X \Rightarrow q\bar{q}'q''\bar{q}'''b\bar{b}X \tag{18}$$

leading to 4-parton and 6- parton configurations, respectively. The hadronic analysis for the top search is complementary to the semileptonic analysis discussed in the previous section, in that for the former we demand that there are no isolated high-$p_\perp$ leptons present in the event sample. Hence the two sets of events can be added to increase the top signal. Clearly, the number of jets seen experimentally depends on the jet definition and the efficiency of the particular algorithm. Like in the previous section we use a UA1-like jet algorithm to define jets; $R_{jet}(\Delta\eta, \Delta\phi) = 0.7$ and $E_{\perp jet} \geq 7\ GeV$ with $\Delta\phi = 12^\circ$ and $|\eta| \leq 3$.

To reduce the background from the NC, CC and $W^\pm X$ events, we impose the cuts $\Sigma E_\perp \geq 120\ GeV$, and $S_{cm} \geq 0.25$, where S_{cm} is the sphericity defined in the hadronic c.m. system. The sphericity distributions from the top quark events and the background processes are shown in Fig. 6. The jet-multiplicity distributions from the NC, CC and $\bar{t}b$ events are shown in Fig. 7. We see that the 4-parton state (from the $\bar{t}b$ events) translates itself into 3-, 4- and 5-jet configurations due to the definition of jets. Based on Fig. 7, we impose a cut on the number of jets, N(jets) ≥ 3, and will concentrate mostly on the 3-jet and 4-jet configurations. We remark that at this stage the $\frac{S}{B}$ ratio is $\frac{650}{4250}$, $\frac{255}{4250}$ and $\frac{142}{4250}$ for $m_t = 150,\ 200,\ 225\ GeV$, respectively. The quality of the top signal can be improved by demanding a cut on the missing $p_\perp$, $\not{p}_\perp \geq 30 GeV$, which effectively removes the NC background (but not the CC and $W^\pm$ events) giving a $\frac{S}{B}$ ratio of $\frac{500}{1410}$, $\frac{190}{1410}$ and $\frac{110}{1410}$ for $m_t = 150,\ 200,\ 225\ GeV$, respectively.

At this stage, an attempt can be made to reconstruct the top quark mass. We do this for the 3-jet and 4-jet event samples separately. Fig. 8 shows the invariant mass $m(jjj)$ distribution for the background and signal plus background event samples, with the indicated cuts and $m_t = 150\ GeV$. The corresponding distributions for $m_t = 200\ GeV$ are shown in

Fig. 9. The S/B ratios corresponding to these configurations are shown in Table 4. For the 4-jet sample, one expects that the b-jet produced in the process $e + p \to \nu + \bar{t} + b + X$ is the softest. Thus, ordering the jets in transverse energy $E_\perp^1 \geq E_\perp^2 \geq E_\perp^3 \geq E_\perp^4 \simeq E_\perp^b$, the $\frac{S}{B}$ ratio can be improved. We show the invariant mass distributions $m(j_1 j_2 j_3)$ for the background and signal plus background event samples in Fig. 10 for $m_t = 150\ GeV$; the corresponding distributions for $m_t = 200\ GeV$ are shown in Fig. 11. This gives: $\frac{S}{B} = \frac{190}{300}, \frac{76}{300}, \frac{42}{300}$ for $m_t = 150,\ 200,\ 225\ GeV$, respectively.

Finally, we show that the $\frac{S}{B}$ ratio can be significantly enhanced (albeit at the cost of rates!) if one demands some minimal b-tagging. In Fig. 12, we show the inclusive cross section for the process $e + p \to (\geq 3) - jets + l^\pm + X$ (with non-isolated lepton) at $\sqrt{s} \simeq 1.26\ TeV$, as a function of the transverse lepton energy cut-off ($p_\perp^l \geq p_\perp^{cut}$). We incorporate the requirement of b-tagging by demanding at least one lepton, with $p_\perp^l \geq 5\ GeV$. The $\frac{S}{B}$ ratio becomes in this case $\frac{166}{104}, \frac{79}{104}, \frac{45}{104}$ for $m_t = 150,\ 200,\ 225\ GeV$, respectively, for the ($\geq$ 3)-jet sample. Invariant mass distributions for $m_t = 150$ are shown in Figs. 13. For the 4-jet sample, with the additional minimal b-tagging requirement mentioned above, the top enriched sample has the $\frac{S}{B}$ ratios of $\frac{71}{18}, \frac{32}{18}$ and $\frac{19}{18}$ for the three m_t values 150, 200 and 225 GeV, respectively, allowing a good determination of m_t, certainly up to $m_t = 200\ GeV$. The resulting $m(jjj)$ distributions are shown in Figs. 14 and 15 for $m_t = 150$ GeV and 200 GeV, respectively.

We would like to conclude this section by summarising the main results. The semileptonic decays of the top quark would allow to search for the top quark in the range of present theoretical interest, namely $100\ GeV \leq m_t \leq 200\ GeV$. This analysis should be able to confirm top quark signals, which probably would have been seen in the pp mode. The hadronic decays of the top quark allow a proper mass reconstruction in terms of the t-quark decay products (jets). Using a UA1-type jet algorithm, top topologies can be gleaned clearly in the 3-jet and 4-jet samples. Since decays of the top quark (almost) always imply the presence of beauty quark, some minimal b-tagging would be helpful. We find that the hadronic analysis (augmented by b-tagging) allows the reconstruction of the top quark in the mass range $100\ GeV \leq m_t \leq 200\ GeV$.

3 Charmed and Beauty Quark Physics at LEP(I)+LHC

We have presented the estimates for the heavy quark production cross sections in ep collisions at $\sqrt{s} \simeq 1.26\ TeV$ in the previous section (see Tables 1 and 2). The cross sections $\sigma(ep \to c + X)$ and $\sigma(ep \to b + X)$, in contrast to the top quark cross section $\sigma(ep \to t + X)$, are completely dominated by the NC process, $\gamma + g \to Q\bar{Q}$, in which the photon is almost real ($Q^2 \sim 0$). Consequently, the scattered electron will be lost in the beam pipe for most of charmed and beauty quark events. So, charmed and beauty hadron events in ep collisions, though basically NC processes, will have to be triggered through the (heavy quark) jet characteristics, namely the associated transverse energy and/or the leptons in the jet(s). The processes, $e + p \to c + X$ and $e + p \to b + X$ provide a very long handle on the minimum values of the variables, Q^2 and Bjorken-x, which can be measured experimentally. This is illustrated in Fig. 16, where we display the $\log(Q^2) - \log(x)$ scatter plot for the process, $e + p \to c + X$ at LEP+LHC, with $\sqrt{s} \simeq 1.26\ TeV$. Clearly, the limits in (x, Q^2) reachable in this figure are of theoretical interest only, since the actual accessibility would be much more restricted due to the trigger conditions, which we shall discuss in a while.

3.1 Profiles of charm and beauty hadrons in ep collisions

In this section, we present an energy-momentum profile of the charmed and beauty hadrons produced in ep collisions and their subsequent decays. We have used the LUND symmetric fragmentation function [49] for the fragmentation of heavy quarks.

$$f(z) = \frac{(1-z)^a}{z} \exp \frac{-bm_\perp^2}{z} \tag{19}$$

This gives an increasingly harder spectrum for heavy hadrons, in agreement with data. In addition, the standard V-A matrix elements have been used for the heavy quark decays. We start by showing the correlation between the heavy hadron energy and its polar angle, measured w.r.t. the beam axis with the proton direction being along $\theta = 180°$, for the charmed $(D, D_s \equiv F)$−mesons and B-mesons. As expected, the most energetic hadrons are along the beam and hence lost. To show this effect quantitatively, we plot in Figs. 17 the energy and polar angle distributions for the charmed hadrons, charged leptons $l^\pm$ and kaons produced in their decays, at $\sqrt{s} \simeq 1.26\ TeV$. The effects of the beam pipe cut on the energy distributions are shown by the shaded histograms. The corresponding distributions for the NC beauty production process $e + p \to b + X$ are shown in Figs. 18. The beam pipe cut in this case also removes the fastest hadrons, which are preferentially produced along the beam direction, though the effect on the cross-sections themselves is not as drastic. We estimate that about 50 % of the $e + p \to c + X$ and 70 % of the $e + p \to b + X$ will survive the stated beam pipe cut. Thus, we expect that at $\sqrt{s} \simeq 1.26\ TeV$, $O(10^9)$ $e + p \to c + X$ and $O(10^7)$ $e + p \to b + X$ events per 1000 pb^{-1} would be produced in the fiducial volume of a detector in ep collisions, with detection capability over the range $|\eta| \leq 3$.

Returning to our discussion of triggers for heavy quark events in ep collisions, we evaluate the effect of successive cuts on the inclusive charmed and beauty hadron production rates. To that end we plot the distribution $\frac{d\sigma}{d\log x_g}$ for NC production of heavy quarks at $\sqrt{s} \simeq 1.26\ TeV$ for the process $e + p \to c + X$ (Fig. 19 (a)) and $e + p \to b + X$ (Fig. 19 (b)). The successive cuts used are:

a) Transverse energy cut on the hadrons inside the fiducial volume of the detector ($E_\perp$ (had.) $\geq$ $10GeV$, $|\eta(\text{had.})| \leq$ 3)

b) Non-isolated lepton(s): $N(l^\pm) \geq 1$, with $p_\perp^l \geq 1\ GeV$.

With these cuts, we estimate that $\sim$ 1.3% of the $e + p \to c + X$ and $\sim$ 23% of the $e + p \to b + X$ events can be measured in the fiducial volume of a detector. This would correspond to a trigger rate of $\sim$ 3 Hz and $\sim$ 1 Hz, respectively, for the charmed and beauty hadron events at LEP+LHC, with a luminosity of $10^{32} cm^{-2} s^{-1}$ in the ep mode. Obvious measurements here include determination of the gluon densities at very small-x_g values, via the inclusive lepton final states and/or J/ψ production, from the dominant process $ep \to c\bar{c}+X \to J/\psi+X$ as well as from the b decays, $e+p \to b+X \to J/\psi+X$. Concentrating on the inclusive lepton state, and using the cutoffs on $\Sigma E_\perp$(had.) and/or $p_\perp^l$ given above, one can read the accessible x_g-values from Fig. 19. We estimate that x_g-values as small as $6 \cdot 10^{-5}$ will be accessible from the inclusive lepton measurements. The corresponding minimum value of x_g, reachable through the final states $ep \to c\bar{c} + X \to J/\psi + X$, has been estimated to be $x_g(\text{min.}) \simeq 3 \cdot 10^{-5}$ in an accompanying report [26].

This highly enriched charmed and beauty hadron data set can be analysed to search for rare and new phenomena. In particular, searches for the flavour changing neutral current

processes in the charmed and beauty hadron decays are topics of obvious interest. Experimental goals here include, among others, measurements of the transitions $D^0 \to l^+l^-$; $D^0 - \bar{D}^0$ oscillations, measured through, for example, the doubly Cabibbo-suppressed decays or $e + p \to l^\pm l^\pm + X$, with only $c \to s$ decay vertices; and, as noted already, the $B_s^0 - \bar{B}_s^0$ oscillation, measured via $e + p \to l^\pm l^\pm + X$, with secondary vertices which would come from the $b \to c \to s$ decays. The quantity χ, defined earlier, can be measured by the (time integrated) inclusive same-sign to opposite-sign dilepton rates. We shall exemplify this class of phenomena through the analysis geared to measure $B_s^0 - \bar{B}_s^0$ oscillation parameter, x_s.

3.2 Prospects of x_s- measurements at LEP(I)+LHC

Since the mixing ratio for the $B_d^0 - \bar{B}_d^0$ is known, a measurement of the corresponding ratio x_s for the $B_s^0 - \bar{B}_s^0$ could be used in a model independent way (up to SU(3) breaking effects) to determine the Cabibbo-Kobayashi-Maskawa (CKM) matrix element ratio $|V_{ts}/V_{td}|^2$, via the relation [50]:

$$\frac{x_s}{x_d} = |\frac{V_{ts}}{V_{td}}|^2 (1 + \Delta) \tag{20}$$

where $\Delta \sim O(SU(3)\ breaking) \sim 0.2 - 0.5$. The above measurement can be combined with the unitarity constraint, $|V_{ts}| = |V_{bc}| \sim 0.04$, to provide a very good measurement of the (otherwise difficult to measure) CKM matrix element, V_{td}. We shall use the present measurement of $x_d \sim 0.65$, and the anticipated value $|V_{td}| \sim \sin(\theta_c)|V_{ts}| \simeq 0.01$, and $\Delta = 0.2$, to get a ball park estimate of x_s. This gives $x_s \sim 24\ x_d \sim 15$. Such a large value of x_s is also expected for $m_t \sim 140$ GeV, a value hinted upon by the recent electroweak analysis, and theoretical expectations that the pseudoscalar coupling constant for the B-mesons has a value ≥ 200 MeV [51]. A value of x_s that large would not lend itself to be culled from time integrated experiments, such as the ones which measure χ_s, and one may have to resort to measurements of the oscillation lengths to determine the mixing ratio $x_s = \Delta M/\Gamma$, for the $B_s^0 - \bar{B}_s^0$ oscillations, to which we now turn.

We recall that the time-dependent measurements of the yield of the "right- sign" and "wrong-sign" components follow the distributions:

$$\tau \frac{dN}{dt}(B^\circ \to B^\circ) \equiv |f_+(t)|^2 = e^{-t/\tau} \cos^2 \omega t \tag{21}$$

$$\tau \frac{dN}{dt}(B^\circ \to \bar{B}^\circ) \equiv |f_-(t)|^2 = e^{-t/\tau} \sin^2 \omega t \tag{22}$$

with $\omega = \frac{x}{2\tau}$. The oscillation period is given by $T_{osc} = \frac{\pi}{\omega} = \frac{2\pi\tau}{x}$. So, using our ball-park estimate we expect sinusoidal oscillations with periods:

$$(T_{osc})_s \sim 0.4\ psec \tag{23}$$

$$(T_{osc})_d \sim 10.0\ psec \tag{24}$$

The cross-section for $c + p \to b + X$ will not be sufficient to measure the oscillation length in the $B_d^0 - \bar{B}_d^0$ sector, but measuring $(T_{osc})_s$ should be possible if proper time resolution of $O(0.1\ psec)$ could be attained. Therefore, for all practical purposes, one could treat only the $B_s^0 - \bar{B}_s^0$ and $B_s^0 - B_s^0$ decay length distributions as sinusoidal, with all others essentially falling exponentially. The oscillation lengths themselves depend on the Lorentz boost and

lifetime, as indicated in Eq. (1). Thus, for $x_s = 15$, $\gamma = 10$, one expects $(\lambda_{osc})_s \sim 1.3$ mm for the $B_s^0 - \bar{B}_s^0$ oscillation, with the corresponding number for the $B_d^0 - \bar{B}_d^0$ oscillation being ~ 3.3 cm. There are three requirements to carry out these kind of measurements:

1. A functional microvertex detector
2. Flavour-tagging B_s^0 and $\bar{B}_s^0$ through hadronic or semileptonic decays
3. A determination of the B_s^0 (or $\bar{B}_s^0$) momentum, as already indicated by the dependence $\lambda_{osc} \sim |p_B|/M_B$.

The resolution of the proper decay time can be considered as resulting from addition of the following errors in quadrature:

$$(\frac{\sigma_t}{\tau})^2 = (\frac{\sigma_d}{d})^2 + (\frac{\sigma|p_B|}{|p_B|})^2 \qquad (25)$$

The error on $(\frac{\sigma_t}{\tau})^2$ has to be brought to the level of a few per cent, in order to well measure the quantity $(T_{osc}/\tau)_s^2 = O(0.1)$. It is also clear that the larger the value of x_s, the smaller is (T_{osc}/τ) and the better is the resolution required on proper time measurements. Here, $\frac{\sigma_d}{d}$ depends (essentially) on the details of the vertex detector, and $\frac{\sigma|p_B|}{|p_B|}$ on the method to measure the B-hadron momentum.

With the (simulated or assumed) proper time resolution and B_s-tagging efficiency, of course, the number of B-hadrons needed to determine a certain x_s can be easily evaluated. The possibilty of measuring x_s at future experimental facilities where large beauty hadron rates are anticipated, and where detectors either already exist or a detector design has been assumed, has been taken up in a number of studies [43]–[47]. Perhaps these numbers are representative for the ep experiments as well, if appropriate detectors can be built for these collisions. We show in Fig. 20 the end result of one such recent studies, which states that for a proper time resolution $\sigma_t/\tau \leq 0.1$, and B_s tagging efficiency of $O(10^{-3})$, at least $O(10^7)$ beauty hadrons will be required to measure $x_s \leq 10$. These requirements on the detectors are necessary conditions to measure x_s. That these are also sufficient depends upon the actual value of x_s, as can be seen in the analysis of Defoix [46].

The oscillation lengths can be obtained by convoluting the functions $(|f_+(t)|^2, |f_-(t)|^2)$ with the energy distributions of the B-hadrons, which have been obtained from the programme AROMA [14]. Since, as discussed earlier, the oscillation period for the $B_d^0 - \bar{B}_d^0$ transitions is very large as compared to the lifetime, we do not show it here. The decay length distribution $\frac{d\sigma}{dl}(e + p \to eb\bar{b} \to B_s + X)$ are shown in Fig. 21 for the right-sign meson (i.e. $\propto |f_+|^2$) for $x_s = 10$, and the assumed B-hadron energy bins indicated on the figures. The corresponding distributions for the wrong-sign B_s meson (i.e. $\propto |f_-|^2$) are shown in Fig. 22.

Next, we concentrate on the processes $e + p \to b + \bar{b} + X \to l^{\pm}l^{\pm} + X$ and $e + p \to b + \bar{b} + X \to l^{\pm}l^{\mp} + X$ involving dilepton final states, and study their yield as a function of the decay length. As stated earlier, the only oscillating components in these distributions are the ones coming from the $B_s^0 - \bar{B}_s^0$ and $B_s^0 - B_s^0$ transitions. They can be separated by subtracting an exponential background, an assumption that has been checked with the help of the Monte Carlo programme. To estimate the smearing effect due to the imprecise measurement of the B_s-hadron energy, we again assume certain B_s-energy bins, hoping that such a precision can be reached experimentally in the dilepton final state. To crudely estimate the effect of

the $\frac{\sigma_d}{d}$ term in Eq. (25), we have convoluted the decay length distributions with a vertex resolution of 100 μm, distributed as a Gaussian. The resulting decay length distributions for the process $e + p \to b + \bar{b} + X \to l^{\pm}l^{\mp} + X$, assuming a beam pipe cut of 100 mrad are shown in Fig. 23. Thus, if the B-hadron energy could be experimentally determined with the assumed accuracy, then the oscillation lengths for the $B_s^0 - \bar{B}_s^0$ can be measured. Again, we reiterate that this pattern rapidly vanishes if either the B-hadron resolution worsens and/or the value of x_s becomes large.

4 Summary

We have discussed at some length the production of heavy quarks in the processes $e + p \to Q + X$ at the LEP+LHC collider assuming $\sqrt{s} \simeq 1.26\ TeV$. The rates for c- and b-hadrons in these collisions are rather robust. With a luminosity of $10^{32} cm^{-2} s^{-1}$, we estimate a measurable rate of ~ 3 Hz, and ~ 1 Hz for the charmed and beauty hadron events, respectively, assuming that events with $\Sigma E_{\perp}$ (had.)$> 10\ GeV$ and having a charged lepton with $p_{\perp}^l > 1\ GeV$, can be triggered over the pseudorapidity interval $|\eta| < 3$. These trigger rates are probably manageable, so that no big data reduction may be necessary. This would make the ep collisions an attractive possibility to do high precision c- and b- physics. We have argued here that the inclusive lepton events, as well as J/ψ-production are very well suited to measure the gluon structure function in very small-x_g region –an area of obvious theoretical interest. As an example of the kind of new phenomena which could be studied at the LEP+LHC collider, we have presented profiles of oscillation lengths associated with the $B_s^0 - \bar{B}_s^0$ transition. The experimental prerequisites for carrying out such measurements have been discussed, and it is argued that a proper time resolution of $O(0.1)$ and an effective B_s-tagging should enable one to measure x_s in the vicinity of ~ 10.

The potential of the ep collider in studying the physics of the top quark is mostly of exploratory nature, since the cross sections for $e + p \to t + X$ are typically in the range of $(5 - 0.5)\ pb$, for the top quark in the mass range $(100 - 250)\ GeV$, providing $\sim (5000 - 500)$ top quark events. To be able to detect these events and construct the top quark mass, we have done two complementary analyses here. In the case of the semileptonic decays of the top quark, the dominant background is due to the production and decays of real W-boson. To suppress this background, one may have to require an additional b-quark tagging, which discriminates the direct W-production (background). This should allow top searches for up to $m_t = 200\ GeV$, and to higher mass if the secondary vertices of the b-quark could be measured with the help of a vertex detector. For the hadronic decay modes of the top quark, the main background is both due to the CC process and the real W-production. Here again, an additional b-tagging would be very helpful. The hadronic events allow the reconstruction of the top quark mass, using the 3-jet decays of the top quark. We estimate that searches of the top quark, certainly up to $m_t = 200\ GeV$, could be successfully undertaken in ep collisions.

Acknowledgements

F.B. would like to thank the Alexander v. Humboldt-Stiftung for supporting his stay at DESY during summer 1990. J.J.vd Bij wants to thank DESY for its hospitality and support

during his stay at DESY, where most of this work was done. J.F.T. would like to thank the binational exchange programme– CICYT, Madrid-KFZ, Karlsruhe– for partially supporting his stay at DESY. We would also like to acknowledge useful discussiōns with Pawel Krawczyk and Herbert Steger on aspects of b-physics, and thank A. Ghinculov for his help with the computer programme for one of the top-backgrounds. This work has partially been supported by BMFT, Bonn, FRG.

References

[1] For a recent review see, for example, Heavy Flavors and High Energy Collisions in the 1-100 TeV Range, Ettore Majorana Int. Science Series, Vol. 44 (1989), A. Ali and L. Cifarelli (Eds.) (Plenum Press, N.Y., 1989).

[2] G.W. Brandenburg (CDF Collaboration), Talk presented at the 5th. Yukawa Memorial Symposium, Nishinomiya, Japan (Oct. 25-28, 1990).

[3] F. Dydak, Talk presented at the XXV Int. Conf. on High Energy Physics, Singapore(August 1990).

[4] D. Haidt, in EPS-High Energy Physics '89, Madrid, Spain(1989), Nucl. Phys. B (Proc.Suppl.)16(1990) 294, F. Barreiro et al. (Eds.).

[5] J. Ellis and G.L. Fogli, CERN Report TH-5817(1990).

[6] P. Langacker, Phys. Rev. Lett. 63(1989) 1920.

[7] N.J. Nodulman, in EPS-High Energy Physics '89, Madrid, Spain(1989), Nucl. Phys. B (Proc.Suppl.)16(1990) 40, F. Barreiro et al. (Eds.).

[8] W. Beenakker et al., DESY Report 90-064(1990).

[9] D. Denegri, in ref. [1].

[10] F. Cavanna et al.– These Proceedings.

[11] T. Rodrigo et al.– These Proceedings.

[12] P. Zerwas et al.– These Proceedings.

[13] J.C. Anjos et al., Phys. Rev. Lett. 60(1988) 1239.

[14] G. Ingelman and G.A. Schuler, Z. Phys. C40(1988) 299.

[15] L.V. Gribov, E.M. Levin and M.G. Ryskin, Phys. Rep. 100(1983) 1.

[16] E.M. Levin and M.G. Ryskin, LNPI-Report 1316(1987).

[17] E.M. Levin and M.G. Ryskin, in Proc. of Workshop on Small-x Behaviour of Deep Inelastic Structure Functions in QCD, DESY, Hamburg, FRG(May 1990); to appear in Nucl. Phys. B (Proc. Suppl.) A. Ali and J. Bartels (Eds.).
P.N. Harriman et al., ibid;

J. Kwiecinski and D. Strozik-Kotlortz, ibid;
W. -K. Tung, and B.R. Webber, ibid.

[18] J. Bartels, G.A. Schuler and J. Blumlein, DESY Report 90-091(1990).

[19] V.N. Gribov and L.N. Lipatov, Sov. J. Nucl. Phys. 15(1972) 78.

[20] G. Altarelli and G. Parisi, Nucl. Phys. B126(1977) 298.

[21] S. Catani, M. Ciafaloni and F. Hautmann, Cavendish Lab., Cambridge Report-HEP 90/13(1990).

[22] J.C. Collins and R.K. Ellis in [17].

[23] G. Abbiendi and L. Stanco, DESY Report 90-112(1990).

[24] E. Eichten, C. Quigg, I. Hinchliffe and K. Lane, Rev. Mod. Phys. 56(1984) 579.

[25] A. Ali et al., in Proc. of HERA Workshop, DESY, Hamburg, FRG, Vol.1 (1988) 393; R.D. Peccei(Ed.).

[26] K.J. Abraham, H. Jung, G.A. Schuler and J. F. de Trocóniz –These proceedings.

[27] M. Danilov, in Proc. of the 1989 Int. Symp. on Lepton and Photon Interactions at High Energies, Stanford, USA, M. Riordan (Ed.) (World Scientific, Singapore, 1989) p. 139.

[28] D. Kreinick, in Proc. of the 1989 Int. Symp. on Lepton and Photon Interactions at High Energies, Stanford, USA, M. Riordan (Ed.) (World Scientific, Singapore, 1989)p. 129.

[29] The Physics Program of a High Luminosity Asymmetric B Factory at SLAC,
D. Hitlin, SLAC Report 353(1989).

[30] Feasibilty Study for a B-meson Factory in the ISR Tunnel,
CERN Report 90-02(1990), PSI Report PR-90-08(1990), T. Nakada (Ed.).

[31] G.J. Feldman et al., in Proc. of the Summer Study on High Energy Physics in the 1990s, Snowmass, Colorado, USA , S. Jensen (ed.) (World Scientific, Singapore, 1989); R.H. Siemann et al., ibid;
D. Cline and C. Pellegrini, ibid.

[32] Proc. of Workshop on Detectors for an Asymmetric B Factory, Max-Planck Institut-Heidelberg Internal Report, MPI-H/1990-V6(1990).

[33] The Design of the Electron-Positron Source for Novosibirsk Phi and B Factories and VEPP-3.4, A.V. Novokhotski, SLAC-AAS-NOTE-56(1990).

[34] B-factories with e^+e^- Colliders,
G. Coignet- Talk at the KEK Topical Conf. on e^+e^- Collision Physics, Tsukuba, Japan, and LAPP-Annecy Report LAPP-EXP-89-09(1989).

[35] An Asymmetric B-factory at KEK,
T. Nozaki, KEK Report 90-68(1990).

[36] J. Tuominiemi (UA1 Collaboration);
R.P. Johnson (ALEPH Collaboration);
J.G. Branson (L3 Collaboration);
Talks presented at the XXV Int. Conf. on High Energy Physics, Singapore(August 1990).

[37] L3 Collaboration (B. Adeva et al.), L3 Preprint # 20 (Nov. 1990).

[38] T. Rohaly, Talk presented at the XXV Int. Conf. on High Energy Physics, Singapore(August 1990).

[39] U. Baur and J.J. van der Bij, Nucl. Phys. B304(1988) 451, and in Proc. of the HERA Workshop, DESY, Hamburg(1988) R.D. Peccei (Ed.).

[40] M. Glück, R.M. Godbole and E. Reya, Z. Phys. C38(1988) 441, Erratum C39(1988)590.

[41] R.A. Eichler and Z. Kunszt, Nucl. Phys.B299(1988) 1.

[42] G. A.Schuler, Nucl. Phys. B299(1988) 21.

[43] P. Roudeau, Orsay Reports, LAL-89-21(1989); LAL-90-47 (1990).

[44] M. Reidenbach, in ref. [32].

[45] L.P. Chen et al., SLD Physics Studies, SLAC Report -354(1989).

[46] C. Defoix, College de France Preprint LPC 90-41(1990) and in CERN Yellow Report: LEP at High Luminosity, CERN(1990).

[47] D. Treille, CERN Report EP/90-30(1990).

[48] G. Ingelman, DESY Report (to be published).

[49] B. Andersson, G. Gustafson and M. Söderberg, Z. Phys. C20(1983) 317.

[50] A. Ali and Z.Z. Aydin, Nucl. Phys. B148(1979) 165.

[51] G. Martinelli, Univ. of Rome & INFN-Sezione di Roma Preprint # 754(1990).

[52] G. Fidacaro –These proceedings.

[53] F. Grancagnolo –These proceedings.

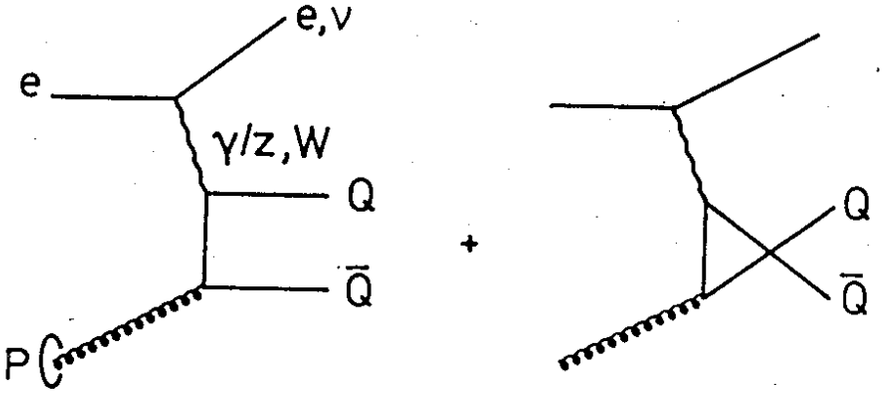

Figure 1

Lowest order boson-gluon fusion diagrams for heavy quark production processes $e + p \rightarrow Q + X$.

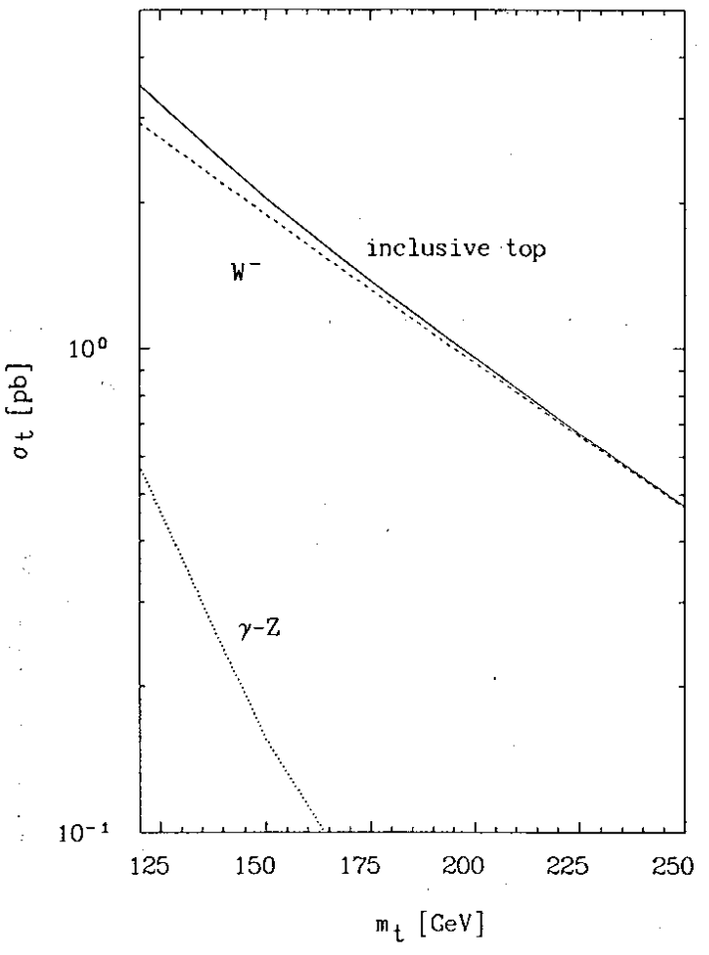

Figure 2

Top quark production cross sections in ep collisions at $\sqrt{s} \sim 1.26\ TeV$; contribution from the NC process $e + p \rightarrow e + t + \bar{t} + X$ (dotted curve), from the CC process $e + p \rightarrow \nu + \bar{t} + b + X$ (dashed curve), and the sum (solid curve), are shown separately.

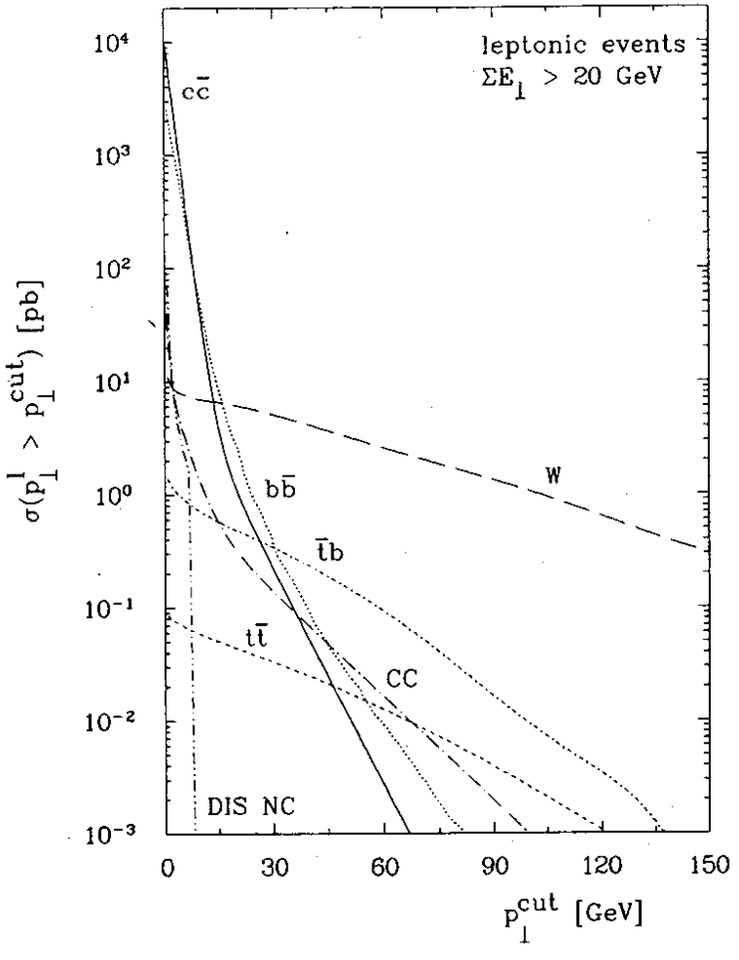

Figure 3

Inclusive semileptonic cross-sections for the process $e + p \to l^\pm + X$ with $\Sigma E_\perp$ (hadrons) $\geq$ 20 GeV as a function of the transverse lepton energy cutoff $p_\perp^l$, at $\sqrt{s} \sim 1.26\ TeV$. The contributions from the top quark (for m_t =150 GeV) and the backgrounds (dominated by NC production of $W^\pm$) are shown individually.

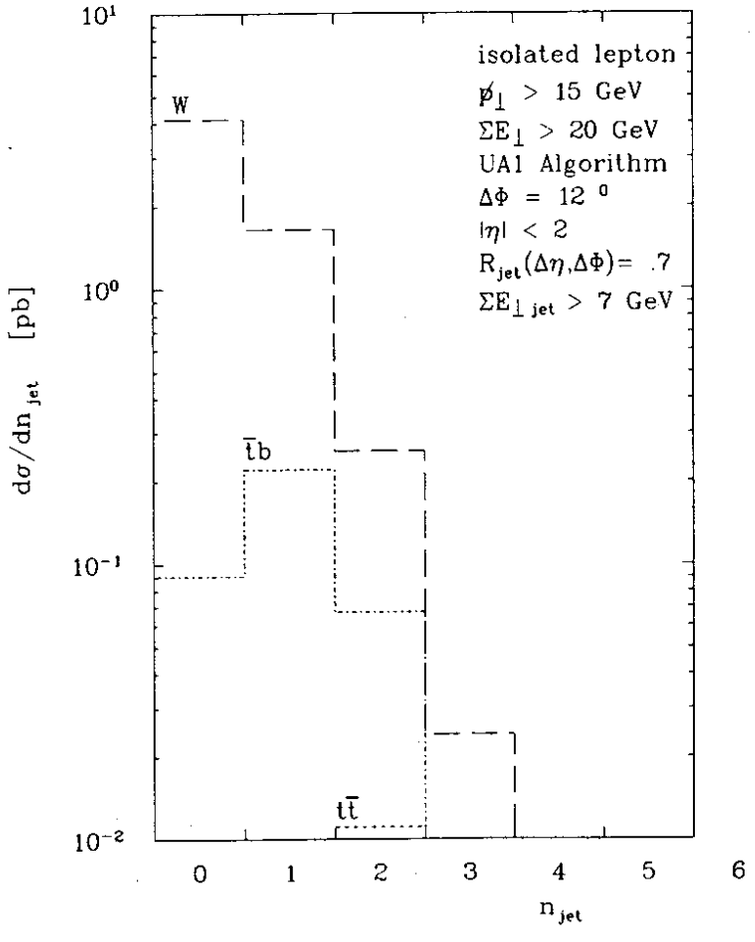

Figure 4

Jet multiplicity distributions in the process $e + p \to l^- + \not{p}_\perp + jet(s) + X$ at $\sqrt{s} \sim 1.26\ TeV$. The definition of jets and additional cuts on the event topology are indicated and m_t = 150 GeV is assumed.

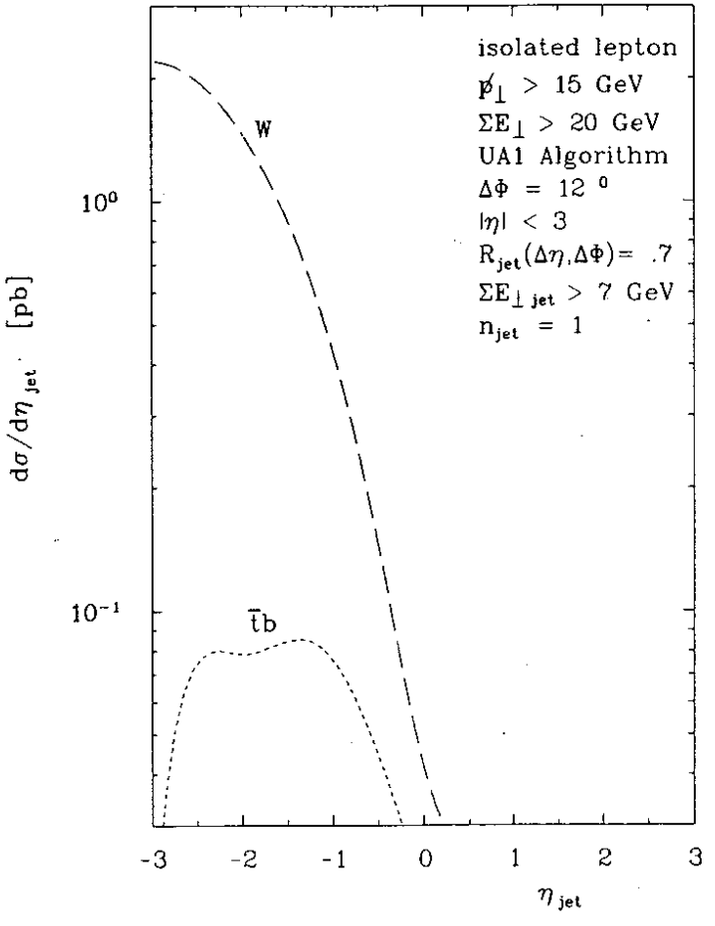

Figure 5

Pseudorapidity distributions for the process $e - p \to l^- + \not{p}_\perp + jet(s) + X$, for $|\eta_{jet}| \leq 3$ from the top quark process (dotted curve) and the dominant background from the NC production of W^- (dashed curve).

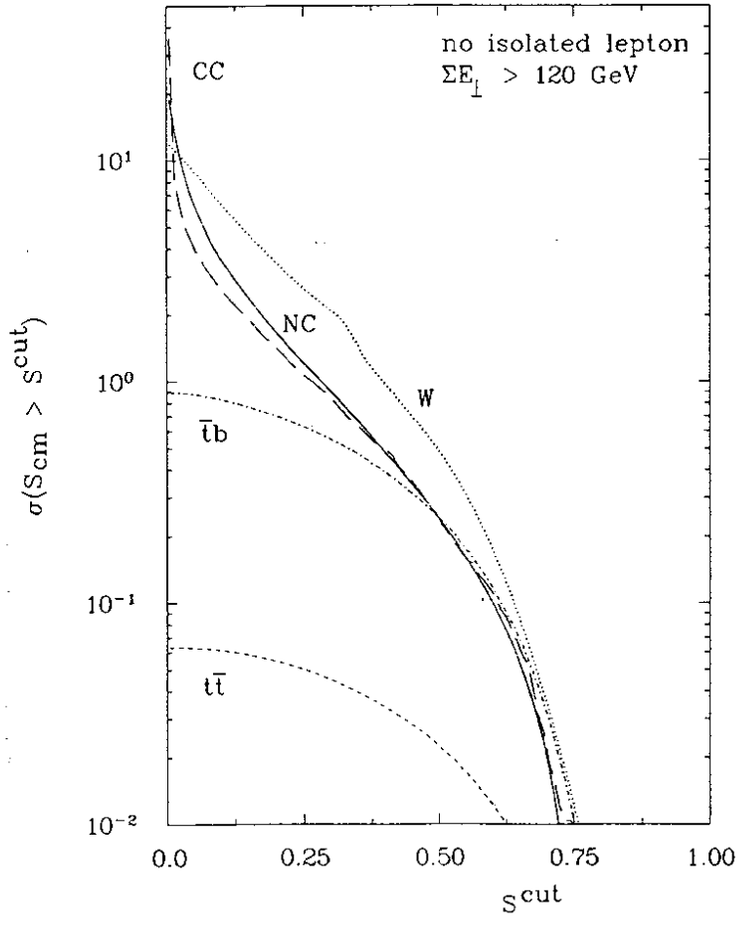

Figure 6

Sphericity distributions for the processes $ep \to jets - X$, with no isolated lepton at $\sqrt{s} \sim 1.26\ TeV$ and $\Sigma E_\perp(had.) \geq 120\ GeV$. The top quark contribution ($t\bar{t}$ and $\bar{t}b$) and background processes are shown.

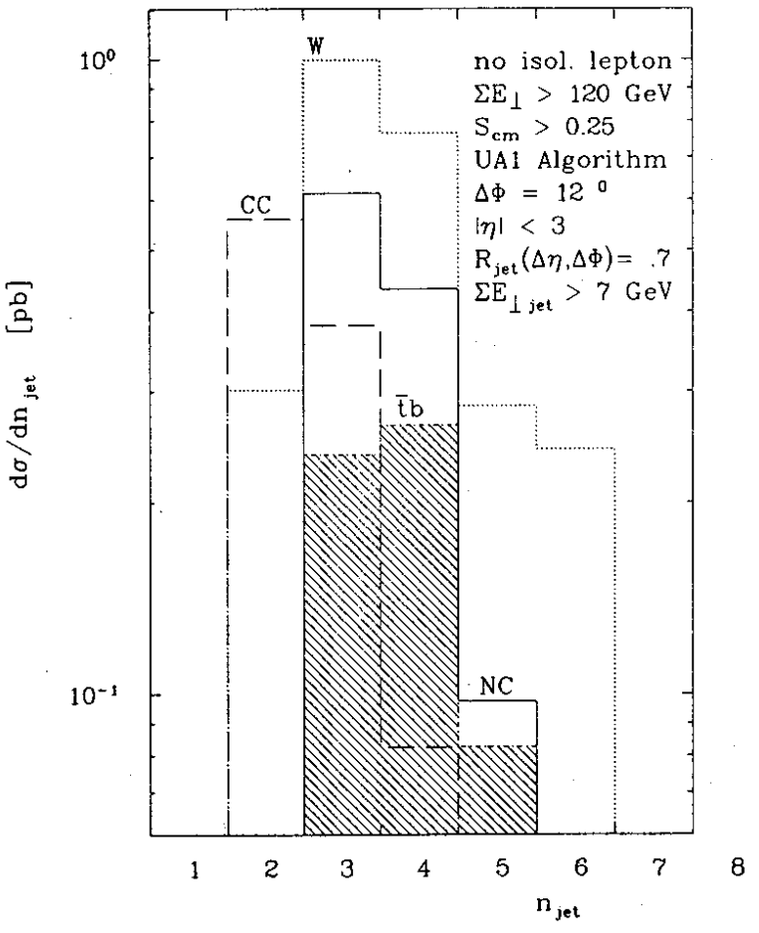

Figure 7

Jet multiplicity distributions in the process $ep \rightarrow jets + X$ for the final states with no isolated lepton, at $\sqrt{s} \sim 1.26\ TeV$. Additional cuts are indicated. The shaded distribution corresponds to the process $e + p \rightarrow \nu + \bar{l} + b + X$. The definition of jets and additional cuts on the event topology are indicated.

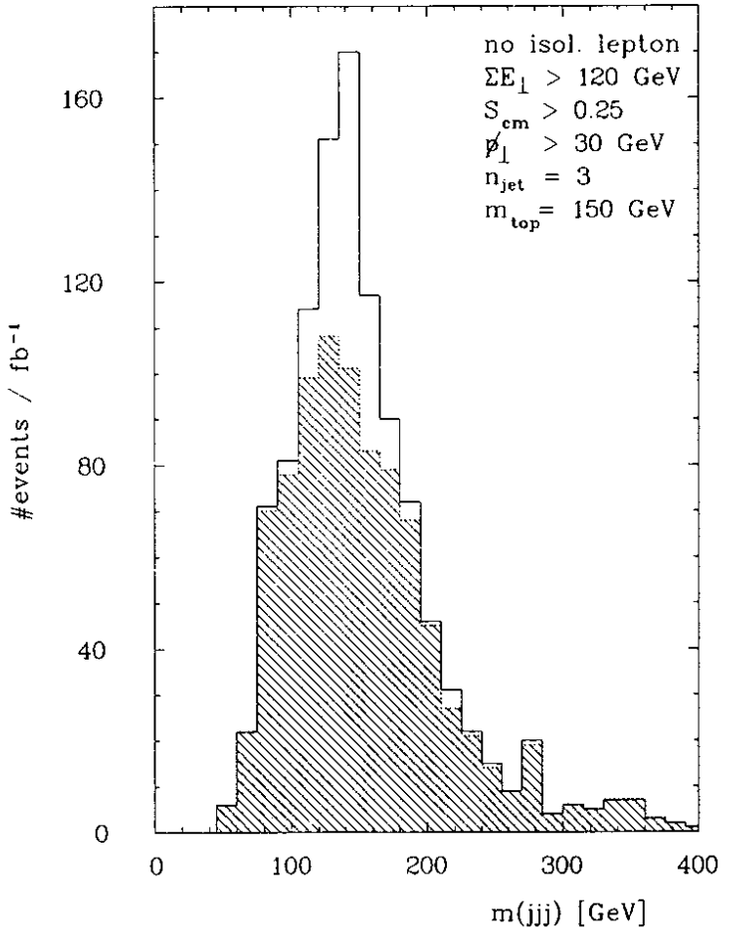

Figure 8

Invariant jet-mass, m_{jjj}, distributions for the process $e + p \rightarrow 3 - jets - X$ with the indicated cuts on the event topology including the top quark contribution (for m_t = 150 GeV), at $\sqrt{s} \sim 1.26\ TeV$. The shaded distribution denotes the background, and the unshaded signal + background.

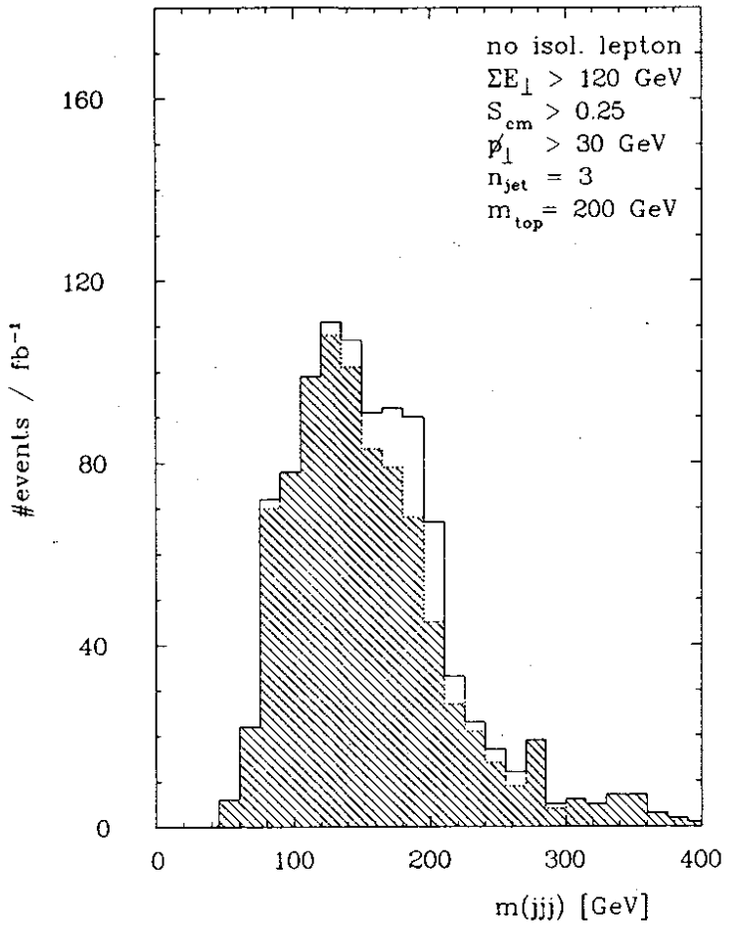

Figure 9

Same as Fig. 8, with $m_t = 200$ GeV.

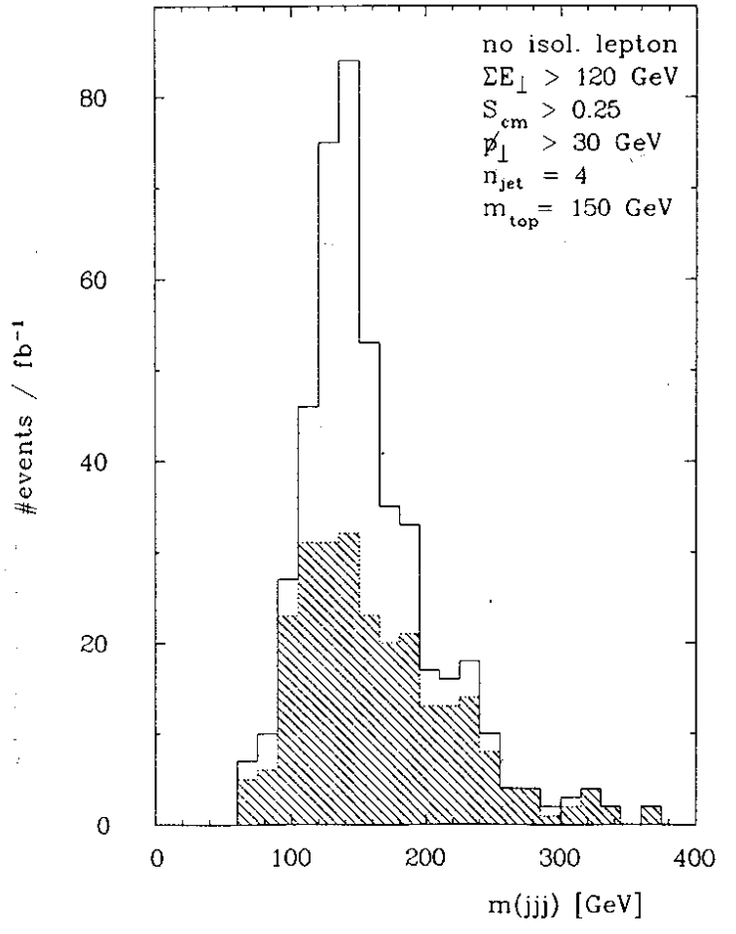

Figure 10

Invariant jet-mass, m_{jjj}, distributions for the process $e + p \to 4 + jets + X$, including the top quark contribution (for $m_t = 150$ GeV), and the indicated cuts on the event topology, at $\sqrt{s} \sim 1.26$ TeV. The jets are ordered in transverse energy and the three most energetic jets have been used to define m_{jjj}. The shaded distribution denotes the background, and the unshaded signal + background.

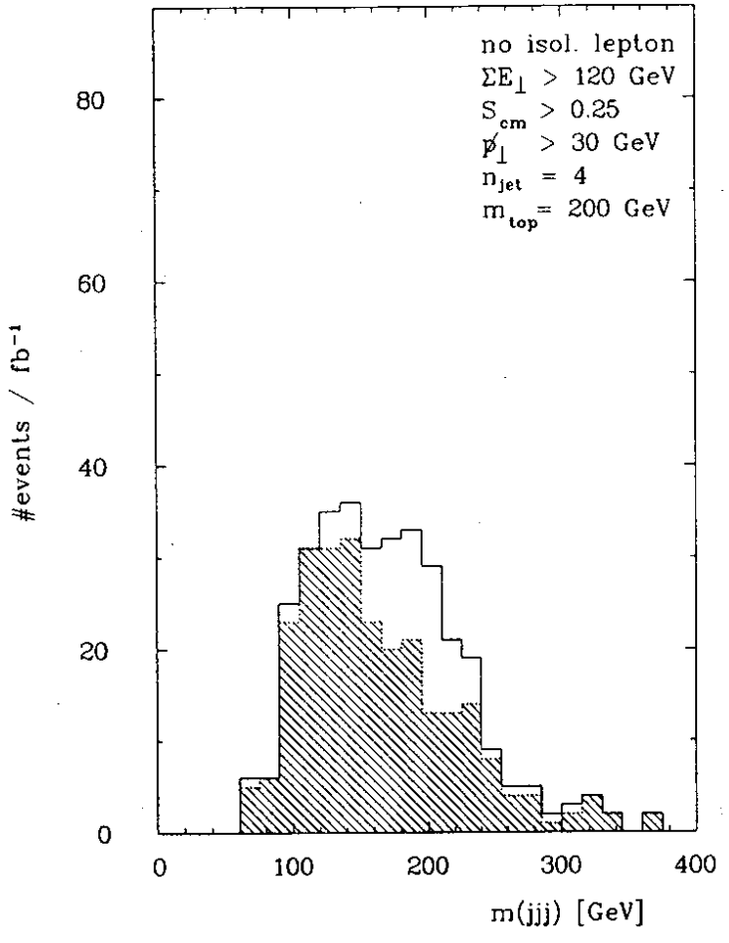

Figure 11

Same as Fig. 10, with m_t = 200 GeV.

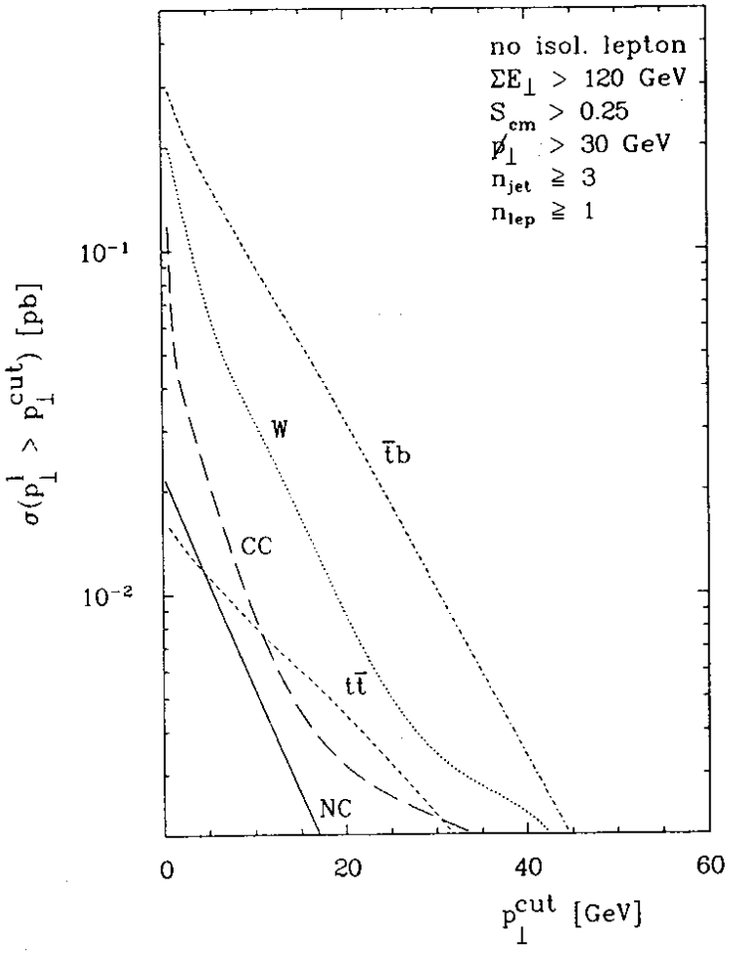

Figure 12

Inclusive cross section for the process $e + p \rightarrow (\geq 3) - jets + l^\pm + X$ (with non-isolated lepton) at $\sqrt{s} \simeq 1.26\ TeV$, as a function of the transverse lepton energy cut-off ($p_\perp^l \geq p_\perp^{cut}$). Additional cuts on the event topology are indicated and m_t = 150 GeV.

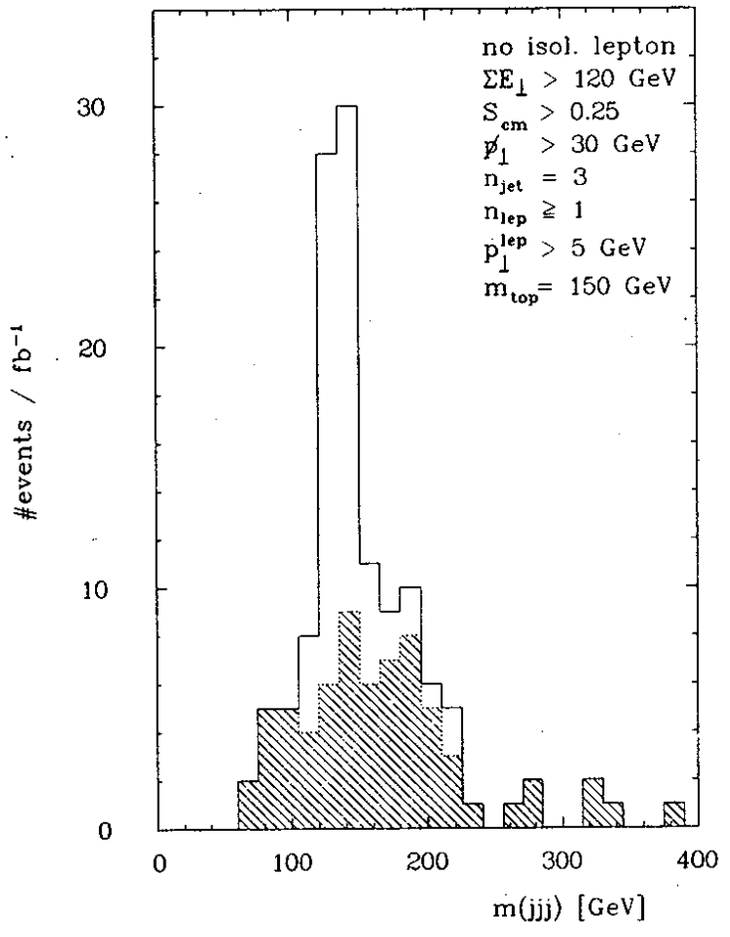

Figure 13

Invariant jet-mass, m_{jjj}, distributions for the process $e+p \to 3-jets+l^\pm+X$, including the top quark contribution (for m_t = 150 GeV) at $\sqrt{s} \simeq 1.26\ TeV$. The lepton(s) satisfy $p_\perp^l \geq 5$ GeV and is(are) not isolated; additional topological cuts are indicated.

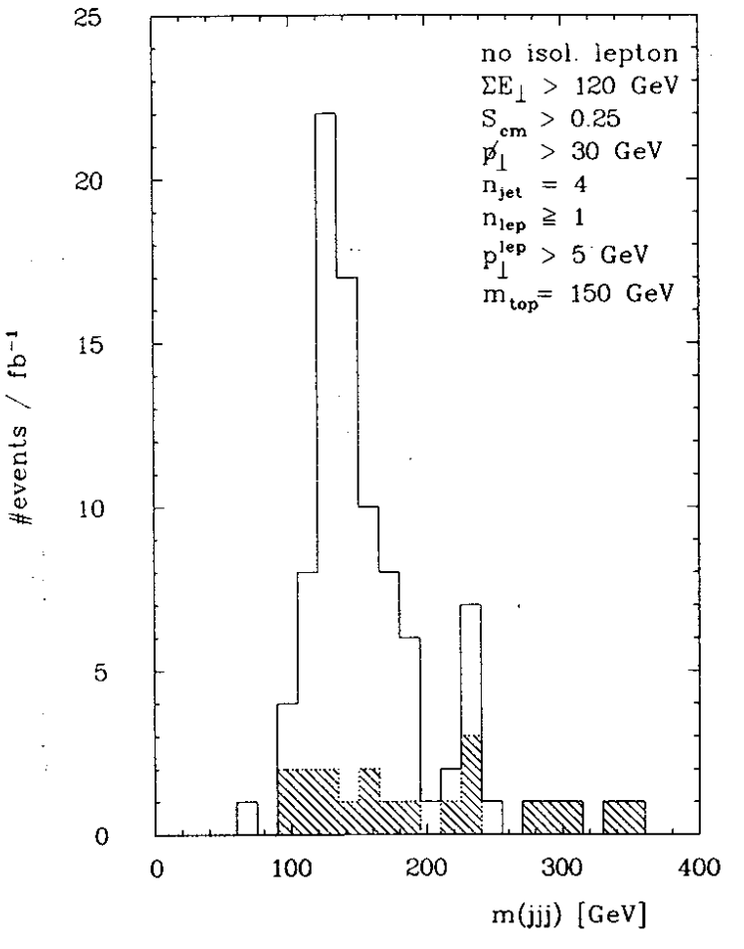

Figure 14

Invariant jet-mass, m_{jjj}, distribution for the process $e+p \to 4-jets+l^\pm+X$ at $\sqrt{s} \simeq 1.26\ TeV$. The jets are ordered in transverse energy and the three most energetic jets have been used to define m_{jjj}. The lepton(s) satisfy $p_\perp^l \geq 5$GeV and m_t = 150 GeV.

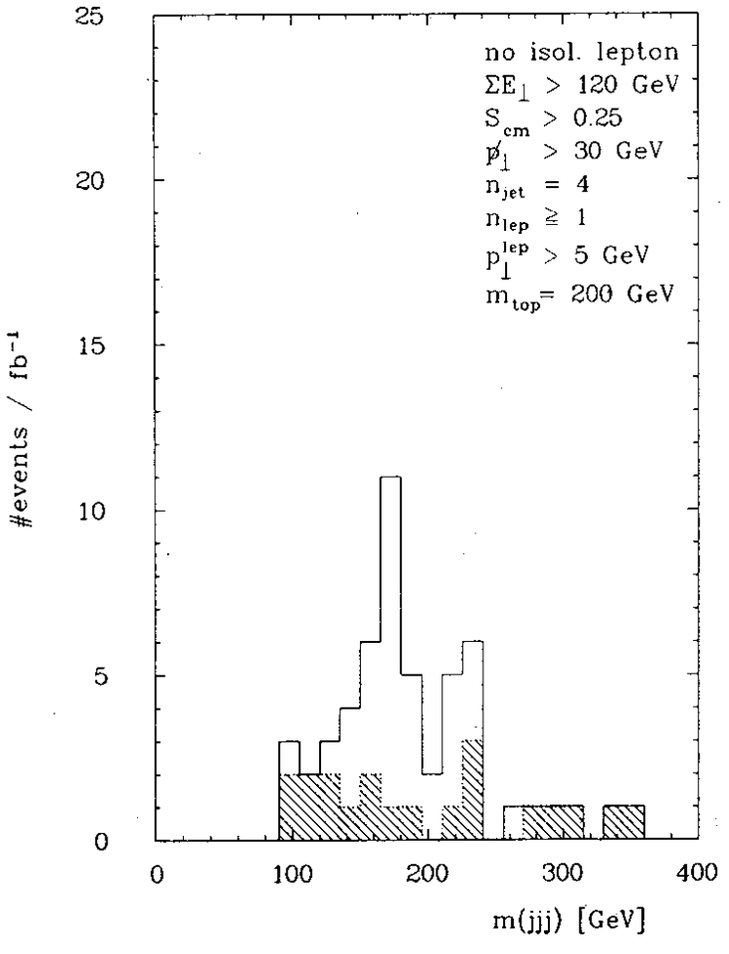

Figure 15

Same as Fig. 14, with $m_t = 200$ GeV.

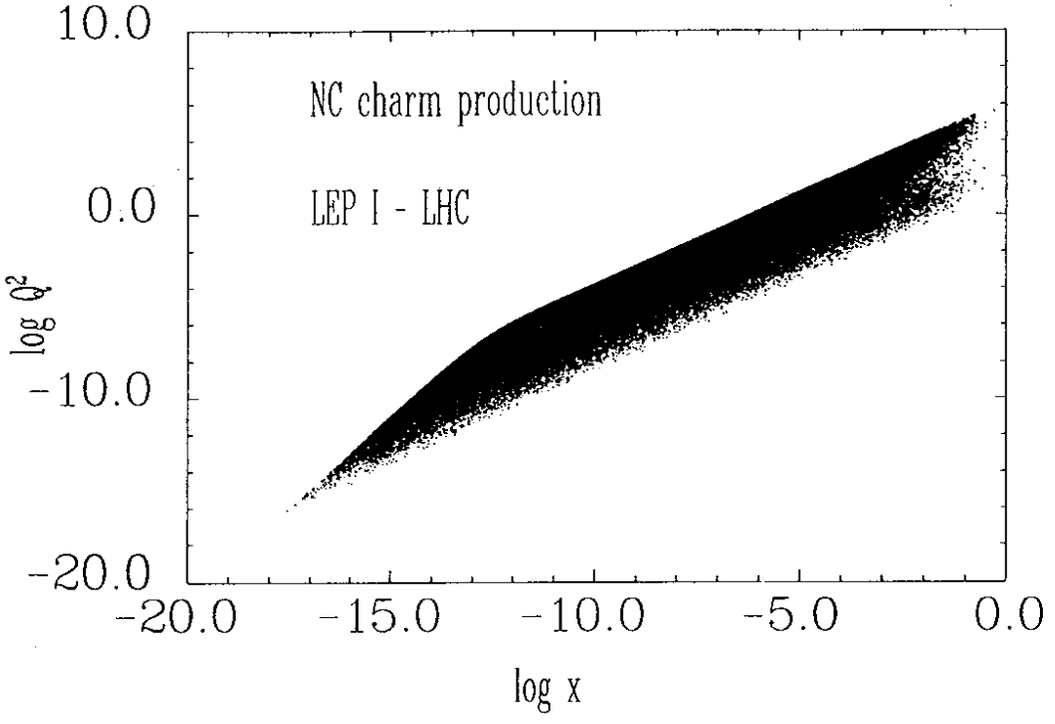

Figure 16

$LogQ^2 - Logx$ scatter plot for the process $e + p \to e - X$ at $\sqrt{s} \sim 1.26$ TeV.

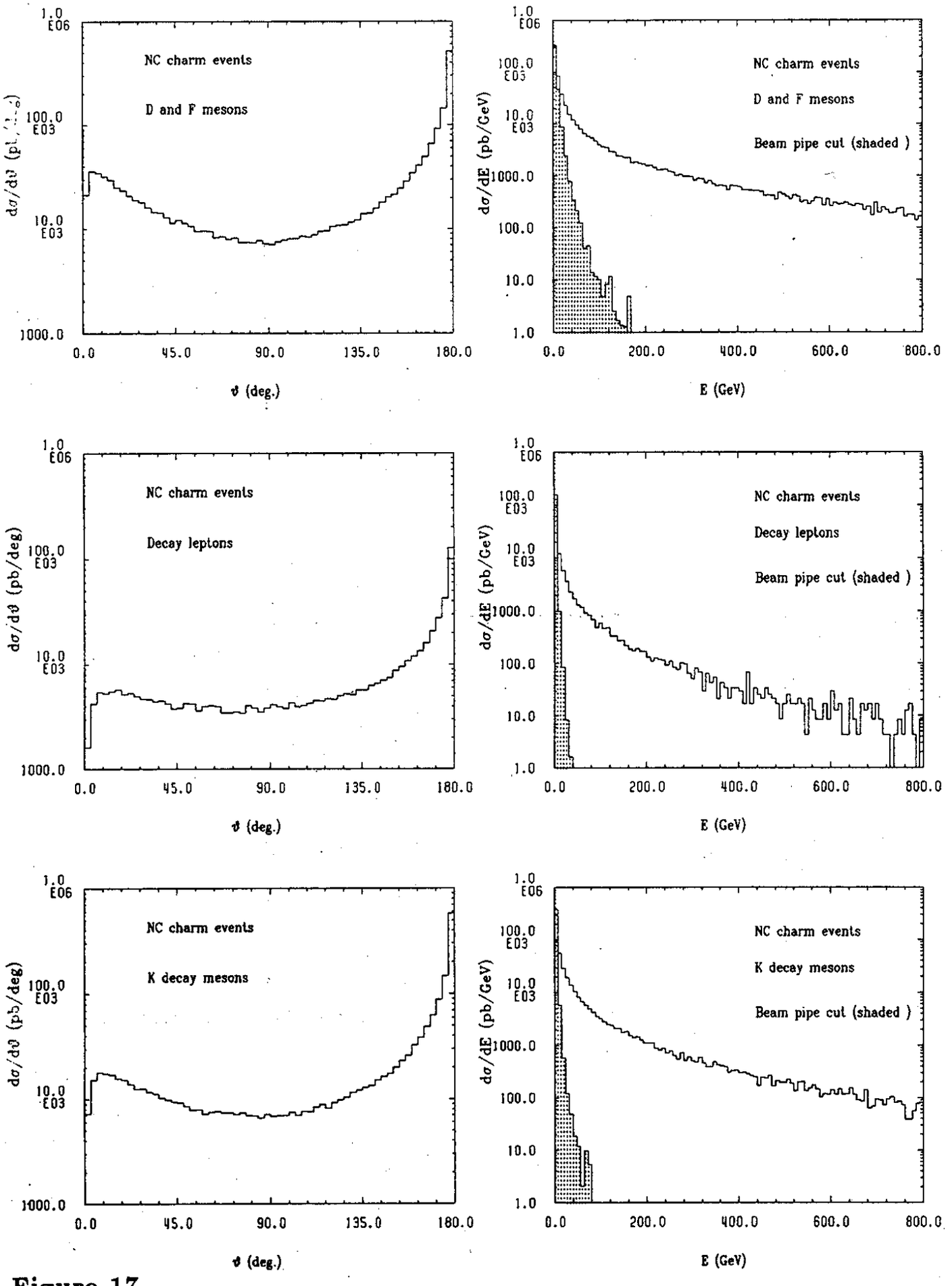

Figure 17

Energy- and Polar angle- distributions for the charmed hadrons D and F ($\equiv D_s$), kaons and charged leptons, produced in the NC process $e+p \to e+X$ at $\sqrt{s} \sim 1.26\,TeV$ and subsequent fragmentation and decays. The energy distributions resulting after imposing a beam pipe cut of 100 mrad are shown by shaded areas.

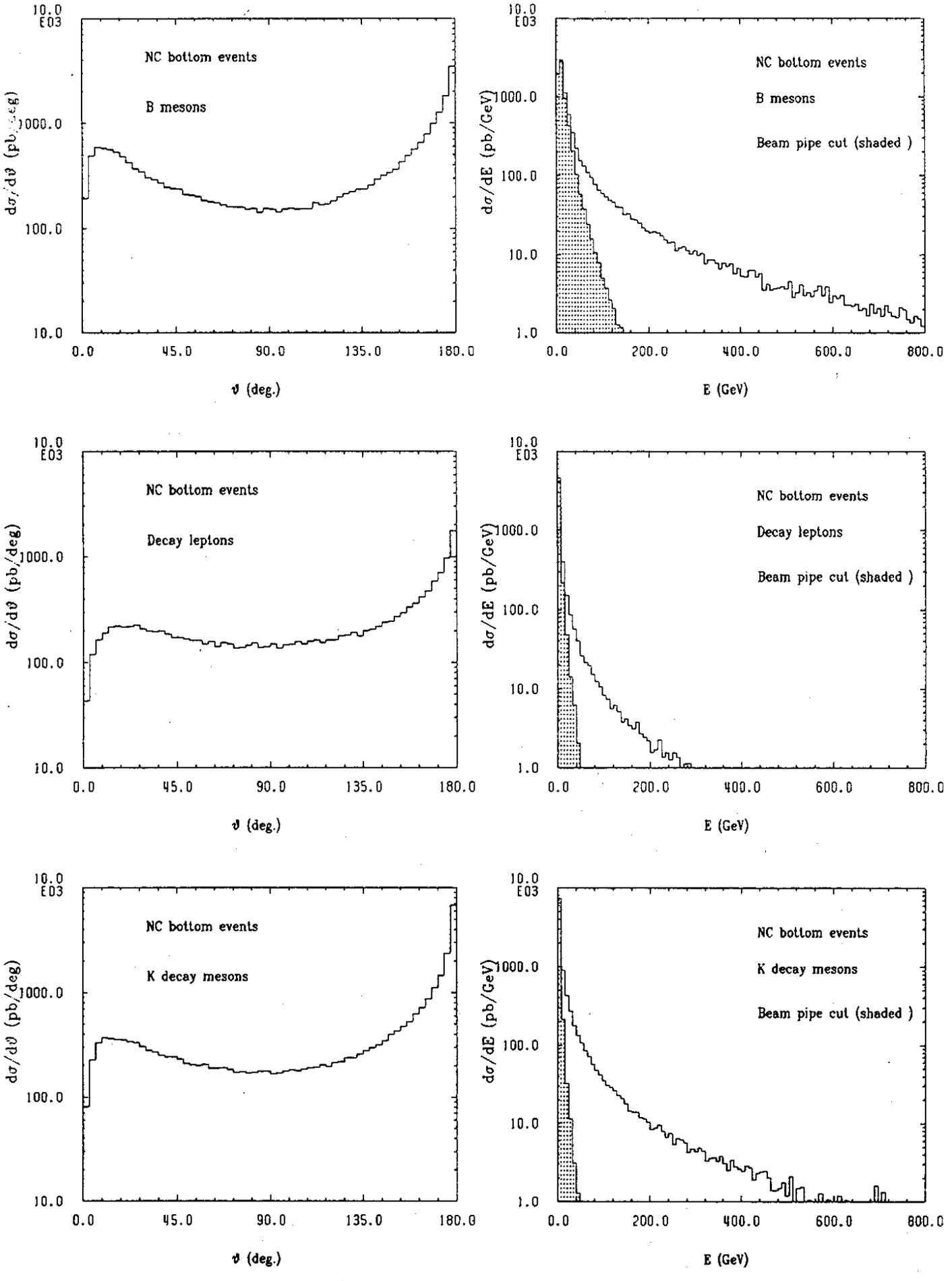

Figure 18

Same as Fig. 17 but for the NC process $e + p \rightarrow b + X$ and involving the B-mesons, kaons and charged leptons.

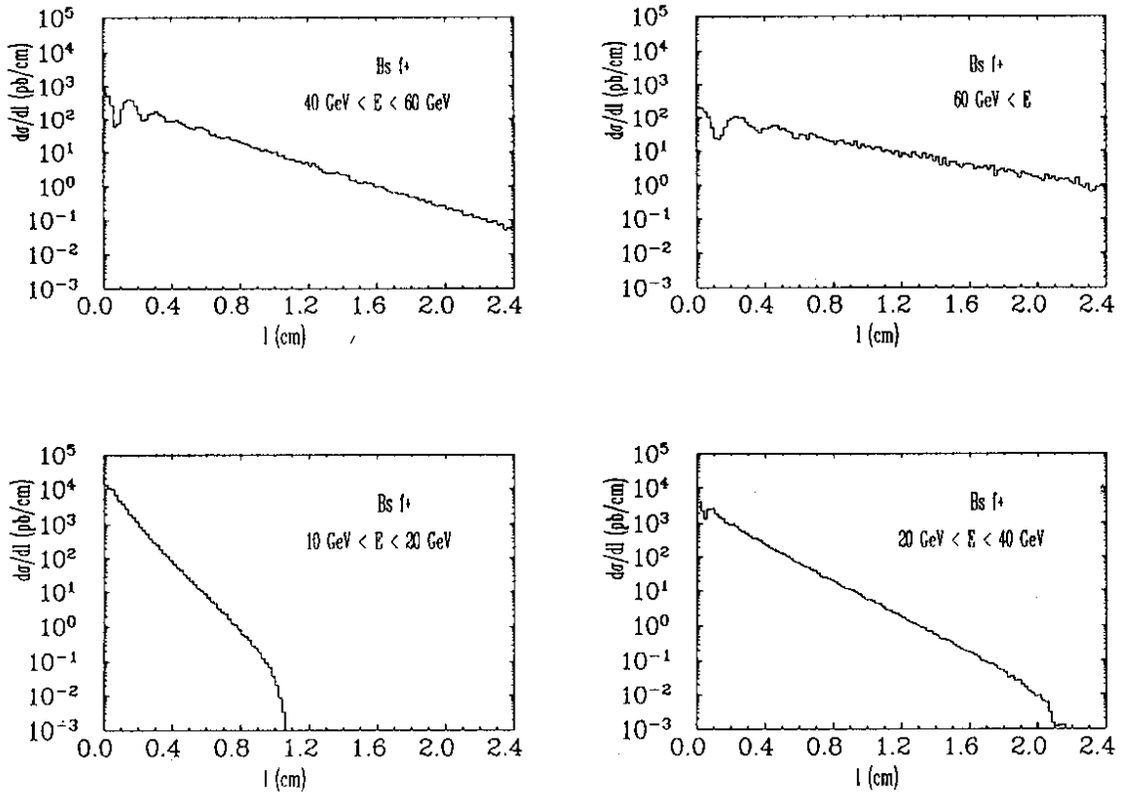

Figure 21

B_s- meson decay length distributions, $\frac{d\sigma}{dl}$ (l in cm) for the right-sign meson transition $B_s^0 - B_s^0$ in the process $c + p \rightarrow b + X$ at $\sqrt{s} \simeq 1.26\ TeV$. An x_s-value of 10 has been assumed and the B_s- meson energy bins are indicated.

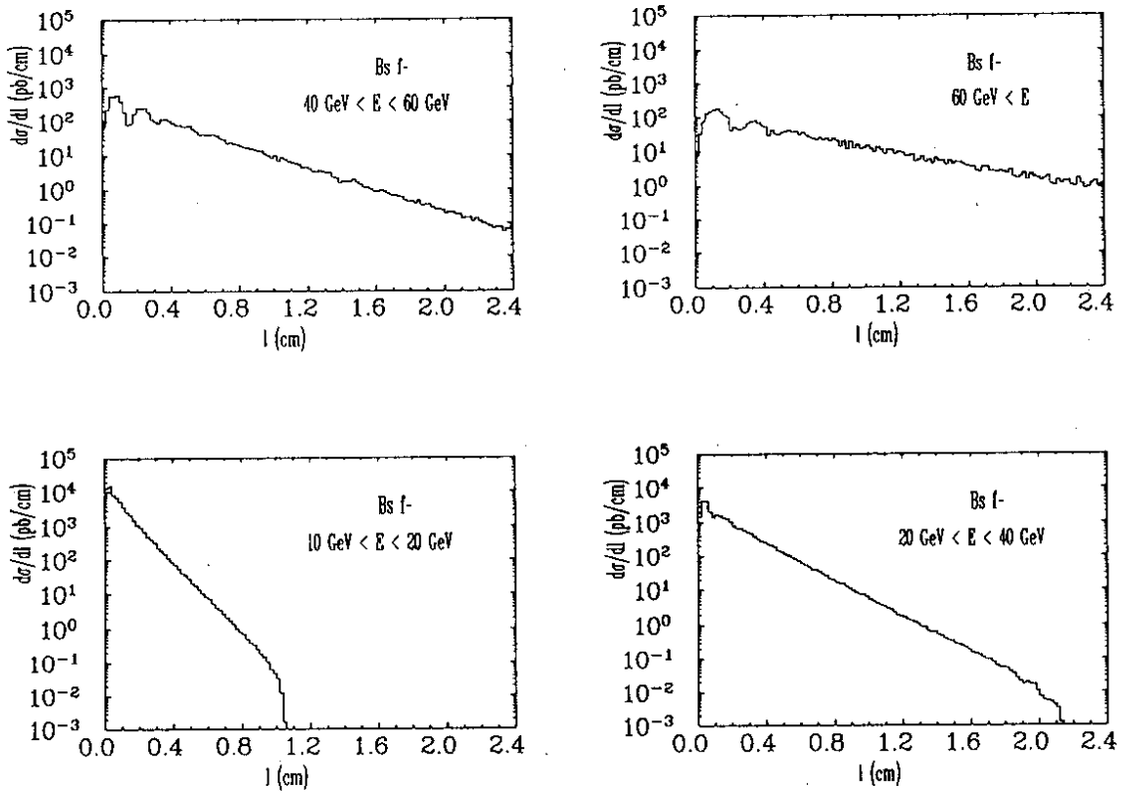

Figure 22

B_s- meson decay length distributions, $\frac{d\sigma}{dl}$ (l in cm) for the wrong-sign meson transition $B_s^0 - \bar{B}_s^0$ in the process $c + p \rightarrow b + X$ at $\sqrt{s} \simeq 1.26\ TeV$. An x_s-value of 10 has been assumed and the B_s- meson energy bins are indicated.

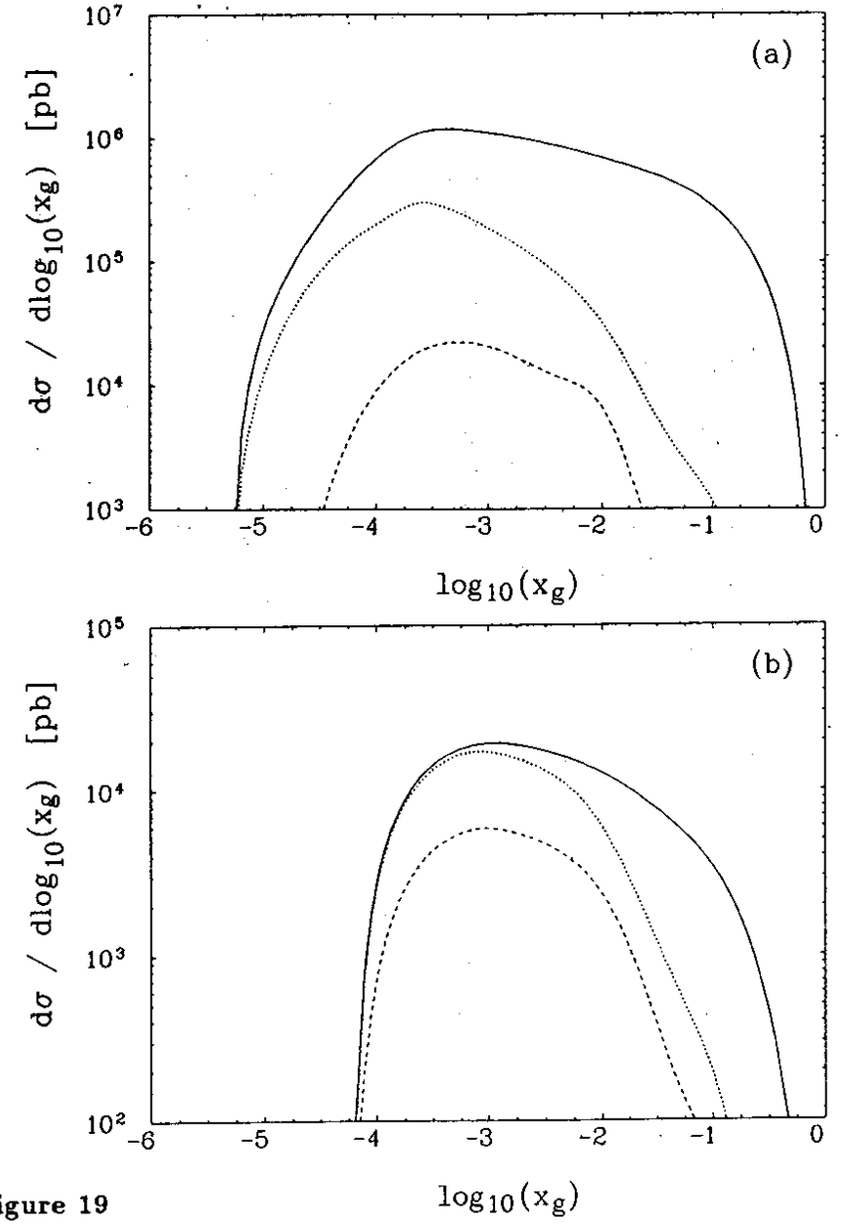

Figure 19

The distribution $\frac{d\sigma}{d\log x}$ for NC production of heavy quarks at $\sqrt{s} \sim 1.26\,TeV$: (a) $e+p \to c+X$ and (b) $e+p \to b+X$. The legends are: No cuts (solid curve). $\Sigma E_\perp$ (had.)$\geq$ 10 GeV (dotted curve), $\Sigma E_\perp$ (had.)$\geq$ 10 GeV and $p^l_\perp \geq 1.0$ GeV (dashed curve), where the lepton is from the semileptonic decay of the charmed and beauty hadrons.

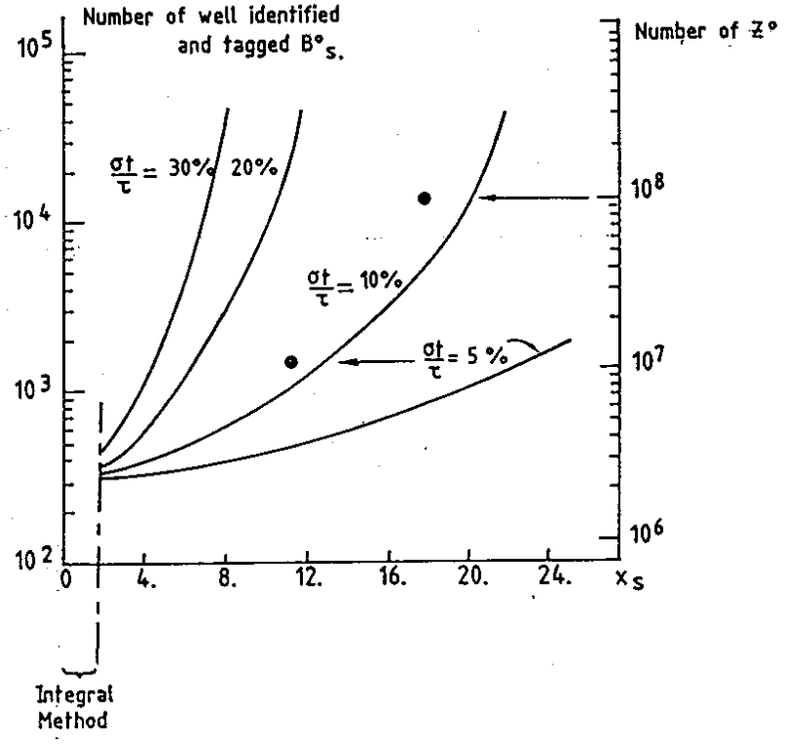

Figure 20

The number of well identified and tagged B^0_s mesons required versus the measurable value of x_s with the assumed proper time resolutions indicated on the curves. The black spots correspond to 10^7 and 10^8 Z^0 events, which would be required at LEP(I) to measure x_s. The required number of B^0_s mesons for the time integrated method are also indicated. Figure taken from ref. [42].

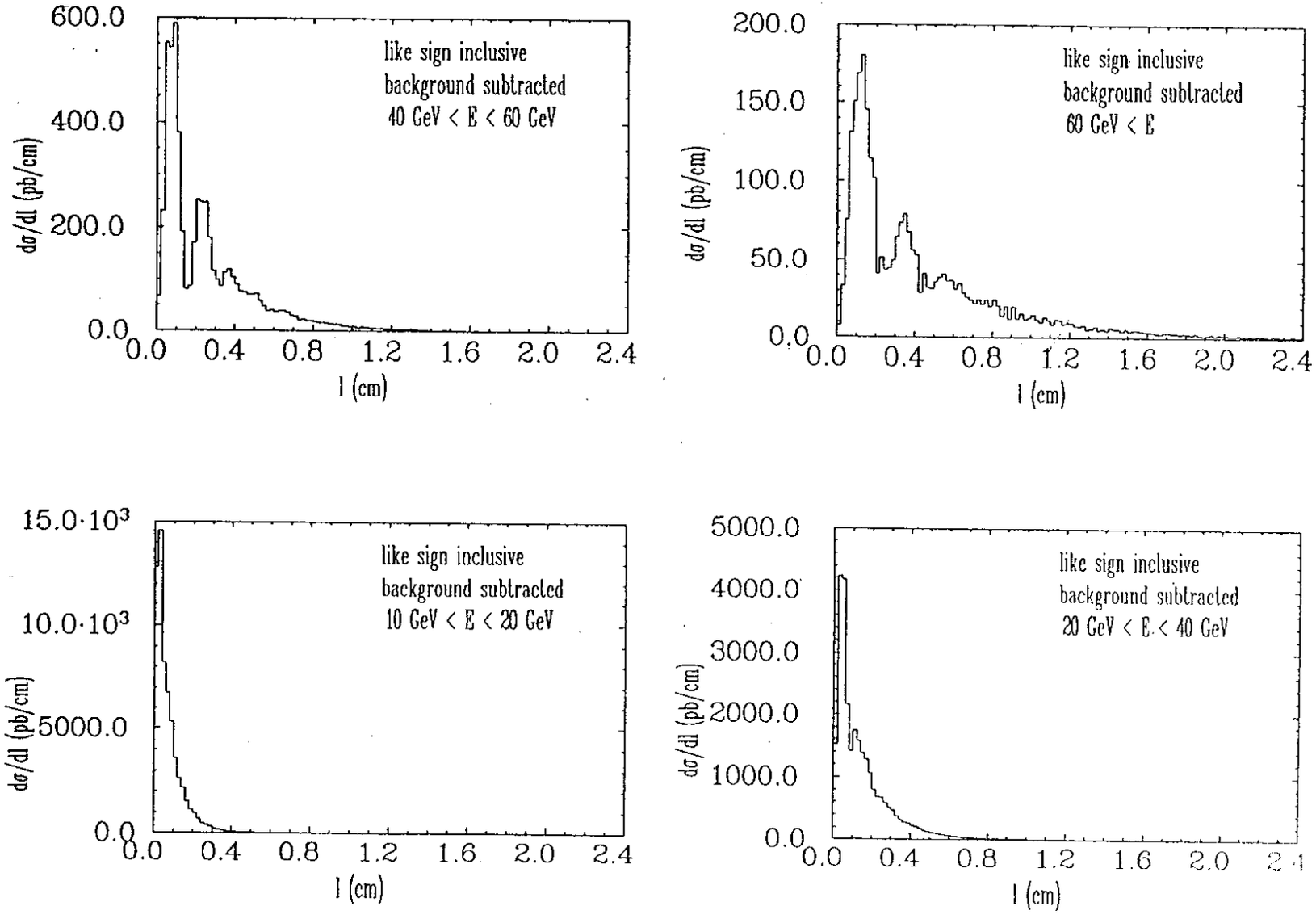

Figure 23

Differential cross section $\frac{d\sigma}{dl}$ (l in cm) for the opposite-sign dilepton process $e + p \to b\bar{b} + X \to l^{\pm}l^{\mp} + X$ cm) at $\sqrt{s} \sim 1.26\ TeV$, after subtracting an exponential background and assuming a vertex resolution of 100 μm. The indicated energy bins on the B_s-mesons are indicated, and a value $x_s = 10$ has been used.